REMARKS

Examiner J. L. Brophy is thanked for the thorough examination and search of the subject Patent Application.

All Claims are believed to be in condition for Allowance and that is so requested.

Reconsideration of the rejection under 35 U.S.C. 102 of Claims 1, 3 and 6 as being anticipated by JP08102489A is requested in accordance with the following remarks.

Applicants' invention provides a means for improving adhesion of a TEOS oxide layer to an underlying low dielectric constant material layer. Silicon ions are implanted into the underlying layer to improve adhesion. As shown in Fig. 2, the silicon implantation is performed on a flat surface. The underlying passivation layer 12 is also a planarizing layer. In JP08102489A, the silicon implantation is performed over non-planar features (See Fig. 1a). JP08102489A teaches implanting silicon ions into a plasma TEOS film to prevent moisture diffusion. Those skilled in the art of microelectronics know that the definition of low dielectric constant means a dielectric constant of less than 3. (See Exhibits A and B). The dielectric constants of the

group of low dielectric constant materials in Applicants' invention: i.e., porous or non-porous carbon-based silicon oxides, porous or non-porous doped silicon oxides, porous or non-porous organic polymers, or porous or non-porous inorganic polymers are all less than 3. (See Exhibit C for doped silicon oxides, Exhibit D for carbon-based silicon oxides, and Exhibit E for organic and inorganic polymers) The dielectric constant of PECVD TEOS is 4 to 4.2 (see Exhibit F). Thus, the material of JP08102489A is not a low dielectric constant material and is therefore different from Applicants' claimed invention.

Reconsideration of the rejection under 35 U.S.C. 102 of Claims 1, 3 and 6 as being anticipated by JP08102489A is requested in accordance with the remarks above.

Reconsideration of the rejection under 35 U.S.C. 102 of Claim 1 as being anticipated by Muroyama is requested in accordance with the following remarks.

Muroyama teaches implanting silicon ions into a thermal oxide film to make its surface hydrophobic. The dielectric constant of undoped silicon dioxide is 4 to 4.2. (See Exhibit F) Thus, the material of Muroyama is not a low dielectric constant material and is therefore different from

Applicants' claimed invention.

Reconsideration of the rejection under 35 U.S.C. 102 of Claim 1 as being anticipated by Muroyama is requested in accordance with the remarks above.

Reconsideration of the rejection under 35 U.S.C. 102 of Claims 1, 3 and 6 as being anticipated by Wantanabe et al is requested in accordance with the following remarks.

Wantanabe et al teaches implanting silicon ions into a spin-on-glass film to decompose its organic components. Organic spin-on-glass appears to fall into the category of low dielectric constant materials of carbon-doped silicon oxide. However, the precursor of (CH3Si(OH)3) (col. 6, lines 31-36) will lead to a final product of carbon-based silicon dioxide plus carbon-doped silanol (with Si-OH bonds). This is well-known for SOG. Furthermore, those skilled in the art of microelectronics will know that the dielectric constant of organic SOG is greater than 3. Thus, the material of Watanabe et al is not a low dielectric constant material and is therefore different from Applicants' claimed invention.

Reconsideration of the rejection under 35 U.S.C. 102 of Claims 1, 3 and 6 as being anticipated by Wantanabe et al is

requested in accordance with the remarks above.

Reconsideration of the rejection under 35 U.S.C. 103 of Claims 4, 5, and 24-27 as being unpatentable over JP08102489A or Wantanabe et al is requested in accordance with the following remarks.

JP08102489A teaches implanting silicon ions into a plasma TEOS film to prevent moisture diffusion. Wantanabe et al teaches implanting silicon ions into a spin-on-glass film to decompose its organic components. As discussed above, low dielectric constant (<3) materials claimed in Applicants' invention are not taught or suggested in the references.

Reconsideration of the rejection under 35 U.S.C. 103 of Claims 4, 5, and 24-27 as being unpatentable over JP08102489A or Wantanabe et al is requested in accordance with the remarks above.

Reconsideration of the rejection under 35 U.S.C. 103 of Claims 3-6 and 24-27 as being unpatentable over Muroyama is requested in accordance with the following remarks.

Muroyama teaches implanting silicon ions into a thermal oxide film to make its surface hydrophobic. As discussed

above, low dielectric constant (<3) materials claimed in Applicants' invention are not taught or suggested in the reference.

Reconsideration of the rejection under 35 U.S.C. 103 of Claims 3-6 and 24-27 as being unpatentable over Muroyama is requested in accordance with the remarks above.

Reconsideration of the rejection under 35 U.S.C. 103 of Claims 12, 14-17, 23, and 28-32 as being unpatentable over Wantanabe et al is requested in accordance with the following remarks.

Wantanabe et al teaches implanting silicon ions into a spin-on-glass film to decompose its organic components. As discussed above, low dielectric constant (<3) materials claimed in Applicants' invention are not taught or suggested in the references. It is agreed that forming a copper layer within an opening is taught in the reference, but this is not a damascene process.

Reconsideration of the rejection under 35 U.S.C. 103 of Claims 12, 14-17, 23, and 28-32 as being unpatentable over Wantanabe et al is requested in accordance with the remarks above.

CS-01-001

Allowance of all Claims is requested.

It is requested that should Examiner Brophy not find that the Claims are now Allowable that she call the undersigned at 765 4530866 to overcome any problems preventing allowance.

Respectfully submitted,

Rosemary L. S. Pike. Reg # 39,332

Attachments: Exhibits A-G

Exhibit A 09/912,737

LOW DIELECTRIC CONSTANT OXIDE FILMS DEPOSITED USING CVD TECHNIQUES

S.McClatchie, K.Beekmann, A.Kiermasz.

Trikon Technologies Ltd., Ringland Way, Newport, Gwent, NP6 2TA, U.K.

ABSTRACT

It has been shown previously that low dielectric constant insulating layers can be deposited using a process technology known as "Low-k Flowfill®". This process uses a chemical vapour deposition (CVD) reaction between methyl-silane (CH_3-SiH_3) and hydrogen peroxide (H_2O_2) to form a methyl doped silicon oxide. Layers deposited using this technique exhibit a dielectric constant < 3.0 and remain stable upon annealing at temperatures of up to 500°C. The layers also exhibit excellent gap-filling capabilities, being able to completely fill 0.1 micron features with up to 4 to 1 aspect ratios. This paper considers the Low-k Flowfill® process in more detail, and examines some of the integration issues that the use of this material raises. The possibility of enhancing the basic methyl-silane/hydrogen peroxide chemistry in order to achieve a lower dielectric constant is also considered. This approach is contrasted with the possibility of using new alternative chemistries in order to achieve dielectric constants values of < 2.5. The use of the pre-cursors dimethyl-silane and methylenebis-silane are considered.

INTRODUCTION

Flowfill® technology, described elsewhere [1-5], utilises a reaction between the simple inorganic precursors silane (SiH_4) and hydrogen peroxide (H_2O_2) to form a flowable SiO_2 that has the ability to fill deep sub-micron features whilst at the same time providing excellent local and a degree of global planarization. The dielectric constant of this material is in the range 3.9-4.4 depending on application. In contrast, the low-k Flowfill® process [6] achieves a dielectric constant of ~2.9 whilst maintaining many of the attractive properties of the original Flowfill® process.

LOW-K FLOWFILL® MECHANISM

The key to the low-k Flowfill® process is the reaction between the gaseous pre-cursor methyl silane (CH_3-SiH_3) and hydrogen peroxide (H_2O_2). Under the correct process conditions these precursor materials react at the surface of the substrate to form what is believed to be a methyl doped silanol type structure. The reaction can be represented in its simplest form by :

$$CH_3\text{-}SiH_3 + H_2O_2 \Rightarrow CH_3\text{-}Si[OH]_3 + \text{by products} \quad \text{.....(1)}$$

Theoretically the CH_3 group does not actively take part in the reaction with the H_2O_2 and as a result remains bonded to the silicon atom. It is postulated that the silanol is then converted into an amorphous methyl doped silicon oxide structure via condensation reactions. This can be represented by:

$CH_3\text{-}Si[OH]_3 \Rightarrow CH_3\text{-}SiO_x + H_2O$ .....(2)

where x = 1.5 - 2.0.

These process steps are depicted in Figure 1. The incorporation of the CH_3 group bound to the silicon atom in the oxide lattice gives rise to the reduction in dielectric constant.

Since the low-k Flowfill® material is formed from gaseous pre-cursors, seamless gap-fill down to 0.1μm, with up to 4:1 aspect ratios can be achieved. The film effectively grows from the bottom-up. At a substrate temperature of 0°C the rate of polymerisation is such that the deposited layer remains a liquid long enough to allow it to flow. As the deposition proceeds and the film grows thicker, surface tension causes the layer to self planarize. The process thus achieves both gap-fill and planarization simultaneously.

Following deposition the layer is subjected to an in-situ heat treatment step in order to promote further polymerisation reactions and convert the material from the liquid form into a stable amorphous structure. An ex-situ furnace anneal (400°C, 30 minutes, N_2 ambient) is then carried out in order to effectively remove any residual moisture that remains as a by product of the polymerisation reactions.

The deposition of the low-k Flowfill® films was carried out using a Planar 200 dielectric deposition tool [1].

PHYSICAL PROPERTIES

Fourier transform infrared (FTIR) analysis revealed the presence of both an Si-C peak at 1275 cm^{-1} and a C-H peak at 2970 cm^{-1} for the methyl doped Flowfill® layers as shown in Figure 3. This confirms the incorporation of the CH_3 group bound to the silicon atom within the silica network.

The thermal stability for the material has been evaluated using FTIR and thermal desorption spectroscopy (TDS) measurements. Figure 5 shows the SiC/SiO and CH/SiO integrated peak area ratios, measured by FTIR, vs. annealing temperature. It can be seen that both the Si-C and C-H bonds remain stable up to annealing temperatures of around 500°C. Figure 6 shows typical thermal desorption spectroscopy (TDS) data for a low-k Flowfill® layer. The data shows that desorption of CH_4 (M/z = 16) and CH_3 (M/z = 15) only occurs at temperatures greater than 500°C, with negligible desorption occurring below this temperature. The thermal stability exhibited by the low-k Flowfill® layer is therefore compatible with existing metallisation schemes.

INTEGRATION

In order to integrate the low-k Flowfill® layer into an inter-metal dielectric scheme it is necessary to deposit a base layer (or liner) prior to depositing the low-k Flowfill® layer. The base layer is a plasma deposited oxide layer which has been optimised to act as a moisture barrier, preventing the possibility of H_2O or H_2O_2 from the Flowfill® layer interacting with the underlying structure. The base also provides a consistent adhesion layer to the overlying low-k Flowfill® layer. An oxide capping layer is then deposited on top of the low-k Flowfill® in order to provide mechanical stability during the final anneal step.

This process sequence gives rise to several integration issues:

Base layer dependence.
The use of a separate liner and capping layer will clearly contribute to the overall dielectric constant of the integrated three layer stack, since the individual layers will act as capacitors in series. The capacitance for an individual layer is given by:

$$C = \frac{k\varepsilon_0 A}{t} \quad \text{.....} \quad (3)$$

where k = dielectric constant, ε_0 = permittivity of free space,
A= capacitor plate area, t=thickness of dielectric.

and the overall capacitance of the integrated stack is given by:

$$\frac{1}{C_{total}} = \frac{1}{C_{liner}} + \frac{1}{C_{lowkFlowfill}} + \frac{1}{C_{cap}} \quad \text{.....} \quad (4)$$

It has been found by experiment that the total capacitance of the three layer stack incorporating the low-k Flowfill® is greater than that given by equation (4). Further investigations have shown that the dielectric constant of the low-k Flowfill® layer is actually dependant on the type of liner it is deposited onto. Low-k Flowfill® layers deposited onto silicon substrates exhibit a dielectric constant of 2.9, however the same film deposited onto a base layer exhibits a dielectric constant of ~3.4. A difference was also observed for low-k Flowfill® films deposited onto a nitride, a silane based oxide and TEOS based oxide which gave a dielectric constant of 3.7, 3.1 and 3.1 respectively. FTIR analysis has shown that the carbon content of the layers is independent of the liner used. This suggests that either the physical structure of the low-k Flowfill® layer has been affected, or that an interfacial effect has been introduced. As the Flowfill® deposition mechanism involves a surface reaction it is reasonable to assume that the condition at the surface of the liner may give rise to either effect. The exact mechanism is currently under investigation.

Since the base layer is required as a moisture barrier, a proprietary surface treatment step has been developed to minimise this effect. The use of the treatment step prior to the low k

Flowfill® deposition reduces the dependence of dielectric constant on the liner and hence the capacitance of the three layer stack to that predicted by equation 4 (Figure 7).

Degassing properties.

As described in a previous section, the low-k Flowfill® layer is subjected to a heat treatment step following deposition using a similar process to that used for the standard SiH_4/H_2O_2 Flowfill® process. This promotes polymerisation of silanols to an amorphous material. TDS has shown that this heat treatment step is insufficient for the low-k Flowfill® layers resulting in incomplete polymerisation. This can give rise to degassing of moisture during subsequent processing steps. The heat treatment step has therefore been optimised resulting in degassing properties similar to those of typical plasma deposited TEOS layers (Figure 8).

The resolution of these issues has allowed the low-k Flowfill® layer to be successfully integrated into 0.25μm technologies [7].

DIELECTRIC CONSTANT OPTIMISATION

The reduction in dielectric constant to 2.9 for the low-k Flowfill® layer has been attributed to the incorporation of the CH_3 group bound to the silicon atom in the oxide lattice. To determine the relationship between dielectric constant and the CH_3 content of the layers the carbon content has been determined using elastic recoil detection analysis (ERDA) and rutherford backscattering spectroscopy (RBS). The dielectric constant was determined by fabricating metal-oxide-metal capacitor structures and measuring their capacitance (f = 1MHz). Figure 9 shows the relationship between dielectric constant and carbon content for the low-k Flowfill® layers. The data was generated by varying the SiH_4:CH_3-SiH_3 gas flow ratio from 1:0 to 0:1. It can be seen that the dielectric constant is dependant on the amount of carbon and hence the number of CH_3 groups present in the layer. It can also be seen that the maximum carbon content that can be achieved repeatably is only ~ 12 at.% which is less that that predicted by the proposed reaction mechanism.

A possible explanation for the lower carbon content is that some of the Si-CH_3 bonds may have been broken as a result of the surface reaction between the CH_3-SiH_3 and H_2O_2. It is possible to achieve a higher carbon content and hence a lower dielectric constant by varying the process conditions, as previously suggested [6], however these process conditions currently give rise to non-repeatability issues. The carbon content can be increased by increasing the process pressure or by decreasing the substrate temperature. The non-repeatability issues arise because both of these changes move the process towards the condensation point of the H_2O_2 precursor resulting in process instability. Current work is centred on further optimising the process conditions to allow a higher carbon content to be achieved.

NEW CHEMISTRIES

An alternative approach to lower the dielectric constant of the low-k Flowfill® films is to modify the process chemistry rather than the process conditions in order to include more carbon. Feasibility studies have shown that this can be achieved by using additional or alternative pre-cursor materials, some of which will now be considered.

Di-methyl silane $(CH_3)_2$-SiH_2 is a gaseous pre-cursor that contains two CH_3 groups bound to the silicon atom as opposed to one CH_3 for methyl silane. Di-methyl silane has been used in addition to methyl-silane to produce a layer with a dielectric constant of ~ 2.75 and properties substantially unchanged from those of the standard methyl-silane process. Matsuura et. al. [7] has taken this process further and shown that it is applicable to sub 0.25μm devices using both W plug and Forcefill® [8] Al plug processes. Device reliability was demonstrated using a 0.25μm two level interconnect scheme. Low via resistance, leakage current and Kelvin resistance, were achieved.

The methyl silane and di-methyl silane based films both result in carbon being bound into the oxide lattice via a Si-CH_3 bond which results in the termination of the siloxane chain. The addition of further CH_3 groups bound to the silicon atom is thought to be prohibitive because an increase in the number of CH_3 groups reduces the number of sites available to form the siloxane chain.

It is possible to incorporate carbon as part of the siloxane chain itself so that the siloxane chain is not terminated. Methylenebis-silane (SiH_3-CH_2-SiH_3) is a gaseous pre-cursor that contains a CH_2 group bound between two SiH_3 groups. The SiH_3 functional groups can take part in the polymerisation reactions with H_2O_2 leaving the Si-CH_2-Si backbone intact as part of the siloxane chain. This precursor has been used in place of methyl-silane to form a layer with a dielectric constant of ~ 2.7.

An alternative approach is to utilise groups other than -CH_3 bound to the reactive -SiH_3 group. By correctly choosing the precursor material dielectric constants in the range 2.25-2.75 are achievable.

The use of alternative precursor materials has demonstrated that the low-k Flowfill® technology can be extended to achieve lower dielectric constants. These results are summarised in Figure 10.

SUMMARY

Optimisation of the CH_3-SiH_3/H_2O_2 low-k Flowfill® process has produced a stable low-k material with a dielectric constant of 2.9, and physical properties that should allow it to be integrated into current metallisation schemes.
Furthermore it has been shown that this CVD technology has the potential to produce a range of new oxide based materials with dielectric constants $\leq$ 2.5 by utilising various organic precursors.

ACKNOWLEDGEMENTS

The authors would like thank K.Giles and the CVD engineering team at Trikon Technologies for their invaluable contributions to this work, and also D.Moore and Dr. P.Timms at the University of Bristol, U.K., for their helpful discussions.

REFERENCES

[1] C.Dobson et al., Semiconductor International, Dec. 1994, pp85-88.

[2] M.Matsuura et al., IEDM, Dec. 11-14th 1994, pp117-120.

[3] M.Matsuura et al, "An advanced planarizing interlayer dielectric using SiH4 and H2O2 chemistry", 1995 Symposium on Dry Process.

[4] A.Hass Bar-Ilan et al, " A comparative study of sub-micron gap filling and planarization techniques", SPIE, Oct. 23rd-24th 1995.

[5] F.Gaillard et al, "Hydrogen peroxide and silane CVD process for pre-metal device applications", DUMIC, Feb. 20-21 1996

[6] S.McClatchie et.al. "Low Dielectric Constant Flowfill® Technology for IMD Applications", DUMIC, Feb. 10-11th 1997.

[7] M.Matsuura et. al., A Reliable Self-planarizing Low-k Intermetal Dielectric for Sub-quarter Micron Interconnects", IEDM, Dec. 7-10th, 1997.

[8] A.J.Mcgeown, "High Pressure Aluminium Fill", ULSI 95, pp. 635-643.

Exhibit B 09/912,737

ULTRA-LOW DIELECTRIC CONSTANTS (ULDC) MATERIALS FOR MICROELECTRONICS AND ETEXTILES

UCLA Technology Available For Licensing

UCLA researchers in the Department of Mechanical and Aeronautical Engineering have developed and reduced to practice a low dielectric material composed of polymers infused with nanoparticles. The material can be used as an interlayer dielectric for large scale integrated interconnects. The material is very thin and has potential application for large area sensing and actuating systems utilizing woven electronic circuits.

Background:
Intensive research is being conducted on low dielectric constant materials. These include fluorinated silica glass, air gap formation, influorinated polymers, polyarythers, inorganic-organic hybrids, porous polymers and other materials. These exhibit dielectric constants in the range of 1.8 to 2.9.

Innovation:
Using specific formulation of polymers and nanoparticles infused into the polymer, a very thin material, on the order of 100 microns in thickness can be fabricated which produces a dialectric constant less than 1.1 at 100 KHz for FE-8% and GNP 4%. Other material systems have been tested and show very low dielectric constants versus competing materials.

The invention makes use of nanofiber technology to create an intense 3-D fibrous network resulting in a fully covered membrane with enormous pore surfaces. The dielectric and mechanical properties of the material can be tailored by selective formulation of the nanoparticle and polymer. The resultant material is produced using electrospinning.

Development to Date:
The dielectric material can be produced in sample quantities and are available for commercial testing. Many combinations of material systems have been processed and tested with the following results all at 100 KHz:

Material	Dielectric Constant
FE 8%	1.08
GNP 4% -A	1.07
GNP 4% -B	1.14
GNP 2% -B	1.16
PAN FE 4%	1.14
FE 1%	1.16
PAN FE 6%	1.16
GNP 2% A	1.18
PAN FE 2%	1.28
PAN (A)	1.46
PAN (B)	1.24

Reference: UCLA Case No. 2003-039

For information on licensing this invention, please contact the ffice bel w.

Office of Intellectual Property Administration
University of California, Los Angeles
10920 Wilshire Blvd., Suite 1200
Los Angeles, CA 90024-1406
Tel: 310-794-0558 Fax: 310-794-0638
email: ncd@resadmin.ucla.edu

NCD URL: http://www.research.ucla.edu/tech/ucla03-039.htm

Lead Inv ntor: Thomas Hahn

Search! Research Interests

UCLA Technologies Available for Licensing
http://www.research.ucla.edu/tech

keywords: therapeutics prophylactic uclancd ucla technologies intellectual property patents technology transfer invention business card

Exhibit C 09/912,737

Flowfill® Technology Low-Dielectric-Constant Materials

Wei-Jen Hsia, Wilbur Catabay, Dung-Ching Perng, & Peter J. Wright, *LSI Logic, Santa Clara, CA, USA*
Liam Cunnane, Knut Beekmann, Simon McClatchie & Adrian Kiermasz, *Trikon Technologies Ltd, Newport, Gwent, UK*

Abstract

The approach to the integration of low-k materials studied in this article is to use an inorganic material such as silicon dioxide doped with organic components. Embedded and non-embedded integration schemes are described. Electrical data shows that the low-k material performs as well as or better than a standard oxide.

Introduction

The integration of organic low-dielectric-constant materials presents the industry with many difficulties. Problems vary depending on the low-*k* material in question, but can include poor adhesion, issues with etching and resist removal creating the potential for via poisoning, and also thermal-conductivity problems with the more esoteric low-*k* films.

The approach studied in this article is to use an inorganic material such as silicon dioxide doped with organic components. The organic content reduces the dielectric constant but the inorganic backbone maintains film properties similar to that of standard silicon dioxide to minimize any integration problems.

Chemistry

The low-*k* flow layer is formed through a condensation reaction between hydrogen peroxide and methylsilane [1], and the addition of silane can be used to control the *k* value. In this way the amount of carbon incorporated into the predominantly inorganic silica film can be adjusted. The maximum carbon content is achieved by complete removal of the silane from the reaction. Water is formed as part of the condensation reaction and a final anneal between 400 and 450°C ensures outgassing and the formation of a high-quality methyl-doped silicon dioxide film.

The low-*k* film exhibits good thermal stability, where carbon loss does not occur until ~ 500°C. Good adhesion is routinely achieved to a variety of materials including Ti, TiN, SiO_2, SiN, and Si. Low stress ~ <5 x 10^8 dynes/cm^2) and unprecedented gap fill properties are also key attributes. Direct chemical-mechanical polishing (CMP) has been carried out with excellent results [2, 3].

Dielectric-constant values as low as 2.7 can be achieved with standard methyl-based chemistry and are directly dependent on the carbon content in the film [1].

Integration Schemes

The Trikon advanced planarization layer typically consists of a plasma-deposited base or liner followed by a low-temperature flow layer, a plasma-deposited cap, and finally a furnace anneal (B-FF-C-FA). The exact functions of the base and cap layers have been reported elsewhere [4]. It is also possible to use a process flow where the Flowfill® is deposited thicker and the cap layer is replaced by a simple treatment step (B-FF-T), hence allowing a lower *k* value to be realized plate to plate as well as line to line; although this is still being investigated to fully understand the process advantages, there are obvious throughput and cost-of-ownership gains. The treatment step, its associated advantages, and film quality aspects will be discussed in a future article. There is some evidence that the base liner layer can be deposited ex situ or indeed possibly omitted, depending on the aluminium passivation and resist strip used during the metal etch (FF-T).

Taking these basic process steps into account, a number of possible integration schemes have been considered, as follows.

Embedded

The embedded approach essentially uses a B-FF-C-FA or B-FF-T sequence deposited over the metal layer. Using either direct CMP or a sacrificial oxide, the structure is CMP'd back to the metal and then capped with a standard oxide. The vias are then etched through the standard oxide layer using usual oxide etch chemistries and all issues to do with low-*k* via poisoning are eliminated. This is clearly not a new idea and has been used with spin-on materials for some time. It does, however, allow a low-*k* CVD film to be used between metal lines without the added difficulty of low-*k* via integration.

Non-Embedded

Both B-FF-C-FA and B-FF-T sequences can be used with this scheme. These process schemes are deposited directly onto the metal structure and vias are etched through the complete stack. Depending on the device metallization, it is possible to use direct or sacrificial polishing exactly as with the embedded approach. Owing to the planarization capability of Flowfill®, it is also possible to delay the use of polishing, or reduce the number of polishing steps in a device. Data has been presented elsewhere which shows improved uniformity, higher throughputs, and reduced CMP consumables when polishing Flowfill, because of its planar nature and the simple fact that less polishing is required to produce the final flat surface [3].

Using a non-embedded approach requires specific expertise and know-how on how to prevent via poisoning in low-*k* films. This can be an expertise in the strip and liner

Figure 1
Scanning electron micrograph of the integrated metal scheme

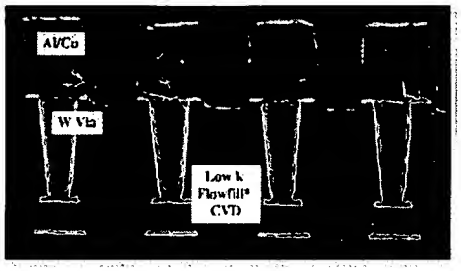

Figure 2
Typical cross-section through a via

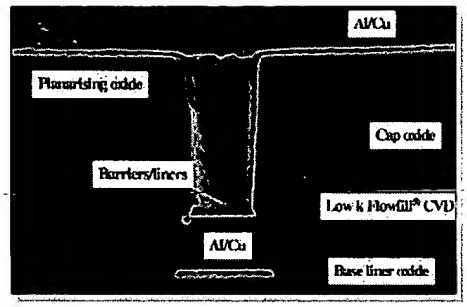

technology or adopting a more complex integration scheme where a hard mask is used to pattern the via, thereby avoiding the use of resist strip chemistries. Typically, the lower the dielectric constant of the low-*k* material, the more difficult it is to prevent via poisoning unless a more complex integration scheme is used. A key advantage of a non-embedded approach is that the low-*k* material can be realized both between the lines and between the metal levels. Clearly a B-FF-T sequence with direct CMP will offer more advantages with respect to *k* value and cost-of-ownership issues than a B-FF-C-FA sequence with a sacrificial CMP layer.

With either the embedded or the non-embedded approach, the base liner can be used ex situ or eliminated as explained above, offering a direct-on-metal (DOM) process.

Figure 1 shows a scanning electron micrograph of the integrated metal scheme. Throughout the work, tungsten plug was used for the via and aluminium/copper alloy was used for the interconnect; 0.18 µm design rules were used, although exact dimensions are proprietary at this stage. Various aspect ratios of both the vias and the metallization in the device can be determined to indicate the complexity of the integration.

In general terms the IMD (Inter Metal Dielectric) process flow was as follows:

1. deposit low-*k* IMD sequence
2. CMP
3. lithography
4. via etch/resist strip/clean
5. degas/deposit liners/W plug
6. W CMP
7. deposit Al
8. lithography
9. etch/resist strip/clean.

Although at first sight the actual dielectric portion of the scheme looks complex, it is in fact relatively straightforward since a B-FF-C or B-FF-T sequence is carried out completely in situ using a predefined process recipe. This is particularly important for ASIC devices, where fast turn-around and minimum process delay times are important. From a processing point of view, only one vacuum break occurs during the complete dielectric deposition; this is between the cap oxide and the planarizing sacrificial oxide if one is used.

Figure 2 shows a typical cross-section through a via. The base-low-*k* Flowfill®-cap structure can be clearly observed. Low-*k* material can clearly be seen both between the metal lines and part way up the via, highlighting the fact that this process is a true *non-embedded* approach.

ELECTRICAL DATA

Wherever possible, electrical data for low-*k* Flowfill® has been compared to a standard oxide, produced by a high-density plasma (HDP) source. In all tests the low-*k* material performed as well as or better than the standard. The singular property which was always better was the capacitance of the IMD layer.

Apart from its gap fill capability, the *k* value of low-*k* Flowfill® can be varied according to the requirements of the device and its design criteria. This offers the possibility for existing devices that use a standard oxide to operate faster, provided the design criteria allow the speed to be realized. The value of dielectric constant can be easily varied from that of HDP oxide ($k \sim 4.2$) to sub-3.0 values. This is done simply by changing the process conditions; no extra hardware is required.

Figure 3 shows the performance of a Kelvin via compared to an HDP oxide.

Figure 4 shows a via chain plot for 0.25 µm vias, again comparing low-*k* Flowfill® to HDP. There is no via poisoning evident, nor indeed any evidence of any high-resistance contacts.

CONCLUSIONS

A flexible low-*k* CVD film has been integrated into a device with 0.18 µm design rules. The physical and electrical characteristics are excellent.

REFERENCES

[1] S. McClatchie, K. Beekmann, A. Kiermasz, and C. Dobson, "Low dielectric constant Flowfill® technology for IMD applications", DUMIC, Feb. 1997.

[2] E. Hartsmannsgruber, M. Kulawski, G. Zwicker and K. Beekmann, "Chemical mechanical polishing of low *k* CVD oxide films", VMIC, Santa Clara, June 1998.

[3] W. Li and G. Sandhu, "Integration of low *k* ILD for reducing digitline capacitance in DRAM", Advanced Metallization Conference, Colorado Springs, Oct. 1998.

[4] C. Dobson, A. Kiermasz, K. Beekmann, and R. Wilby, "Advanced SiO_2 planarization using silane and H_2O_2", Semiconductor International, Dec. 1994.

ABOUT THE AUTHORS

Wei-Jen Hsia has a BSc in chemical engineering from Cooper Union and also an MSc in material science from Stanford University. He has been with LSI, Santa Clara R&D for 11 years and is the Staff Process Development Engineer.

Wilbur Catabay has previously worked for Hewlett Packard and Fairchild Semiconductor and has now been with LSI Logic for 15 years, (SEMATECH for 2 year assignment). He is the Intercon-

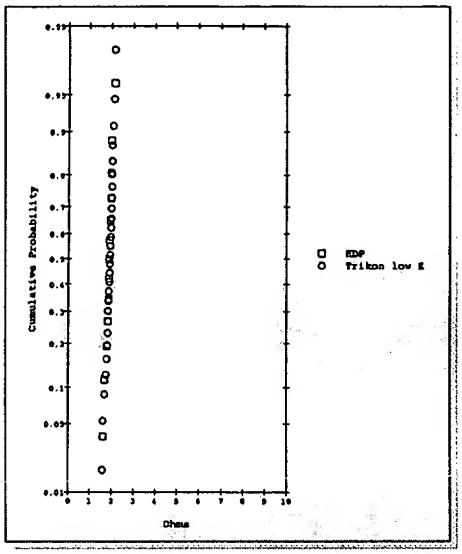

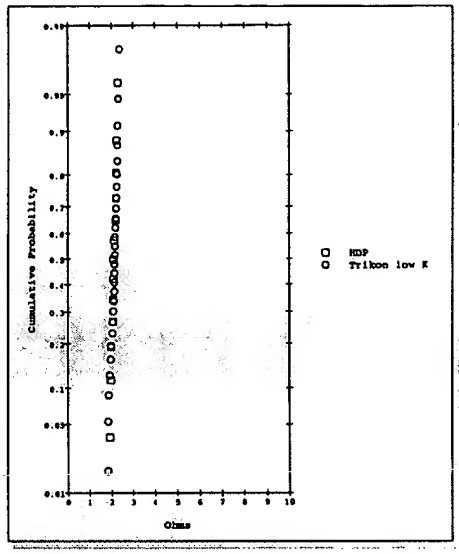

Figure 3 (far left)
Electrical data for a Kelvin via compared to an HDP oxide

Figure 4 (left)
Via chain plot for 0.25 µm vias

nect Manager at Santa Clara Research and Development. He gained a BS Industrial Technology from San Jose State University.

Dung-Ching Perng received his BS, and MS degrees in Physics from National Cheng-Kung University, Taiwan and University of Arizona, Arizona, respectively. He received his PhD degree in Electrical Engineering in 1994 from University of Illinois at Chicago, Illinois. From 1994 to 1996, he worked as thin film development engineer at Applied Materials, Santa Clara, CA. From 1996 to 1997, he worked at Siemens Components, Hopewell Junction, NY, where he worked with IBM and Toshiba personnel to develop 1Gb DRAM in the area of dual damascene oxide etch, gate stack integration. Since 1997, he has been with LSI logic, Santa Clara, CA, where he is a low K process integration engineer for 0.18 um product.

Peter J. Wright received the BS and ME degrees in electrical engineering from Rensselaer Polytechnic Institute, Troy, NY, in 1983 and 1984, respectively, and the PhD degree in electrical engineering in 1989 from Stanford University, Stanford, CA. From 1989 to 1994, he held positions with Texas Instruments, Dallas, TX, where he worked in the areas of plasma etching and multilevel metal for VLSI. From 1994 to 1998, he held positions with Altera Corp., San Jose, CA, where he worked on EEPROM devices for PLDs. Since 1998, he has been with LSI Logic, Santa Clara, CA, where he is the Process Development Manager for the 0.18µm backend integration.

Liam Cunnane is currently the US CVD Manager (Field Support) at Trikon. He gained a BSc Honors UCD from Dublin, Ireland in 1987. He joined Electrotech/Trikon Technologies in October 1988, as a process engineer, supporting all three products CVD, Etch & Sputtering, specialising in CVD in September 1997.

Knut Beekmann graduated in 1984 from Sheffield university with a BSc (Hons) in physics. He left university to work for the CVD division of Electrotech/Trikon Technologies as a process engineer. He is currently the process manager of the CVD group and is responsible for research and development of dielectric deposition and field process support.

Simon McClatchie studied Physics at the University of Wales, Cardiff, where he received a BSc., and later a PhD He worked briefly as a research associate before joining Trikon Technologies as a process engineer in 1994, where he has been engaged in the development of various CVD based technologies. He has over 10 years experience in the semiconductor industry and has authored and co-authored numerous papers. He currently holds the position of technical marketing manager for CVD products.

Adrian Kiermasz was educated at Liverpool University and holds a bachelors degree in physics, a masters degree in device physics and a PhD in plasma physics. His professional qualifications also include Chartered Engineer and Chartered Physicist status. He is the author of over 50 articles in various topics relating to semiconductor technology and is also the holder of several patents in Chemical Vapour Deposition and Low k dielectrics. Currently Dr Kiermasz is Vice President of Semiconductor Technology at Trikon Technologies.

IF YOU HAVE ANY ENQUIRIES REGARDING THE CONTENT OF THIS ARTICLE, PLEASE CONTACT:

Dr Adrian Kiermasz
Trikon Technologies Ltd
Ringland Way
Newport
Gwent, UK

Tel: +44 (0)163 341 4164
Fax: +44 (0)163 341 4125
E-mail: adrian.kiermasz@trikon.com

[Reader Ref. 38]

JOURNAL OF APPLIED PHYSICS VOLUME 90, NUMBER 5 1 SEPTEMBER 2001

Origin of low dielectric constant of carbon-incorporated silicon oxide film deposited by plasma enhanced chemical vapor deposition

Jin Yong Kim
Inter-university Semiconductor Research Center, Seoul National University, Seoul 151-742, Korea

Moo Sung Hwang, Yoon-Hae Kim, and Hyeong Joon Kim[a)]
School of Materials Science and Engineering, Seoul National University, Seoul 151-742, Korea

Young Lee
R&D Division 3, Jusung Engineering Co., Ltd, Kwangju-Gun 464-890, Kyunggi-Do, Korea

(Received 22 February 2001; accepted for publication 4 June 2001)

Dielectric properties of carbon-incorporated silicon oxide (SiOC) films deposited by plasma enhanced chemical vapor deposition (PECVD), using a bis-trimethylsilylmethane precursor, were compared with the dielectric properties of silicon oxide thermally grown in a furnace (thermal oxide) and also with oxide deposited by PECVD using a tetraethoxysilane (TEOS) precursor (PE-TEOS oxide). The electronic contribution to the dielectric constant of the three oxide films was calculated from their refractive indices measured at 632.8 nm by ellipsometry. Ionic contributions were computed from their IR reflection spectra, measured at 650–4000 cm^{-1}, by using the Kramers–Kronig relation. The dipolar contribution was qualitatively analyzed from temperature dependence of the polarizability, on a per unit volume basis. The dielectric constant of the SiOC films, which was measured at 1 MHz, decreased from 4.2 to 2.3 as the carbon content increased from 0 to 19.6 at.%. Although there was a significant reduction of the dielectric constant, the electronic contribution was only slightly changed from 2.10 to 1.90, whereas the ionic polarization noticeably changed from 1.86 to 0.25. SiOC films showed considerable dipolar contribution when compared to thermal oxide and PE-TEOS oxide films, but the dipolar contribution in the SiOC films became negligible as the carbon content was increased. The variation of each contribution with the carbon content shows that carbon incorporation leads to a decrease in the electronic and ionic contributions. The reduction of the ionic contribution was the predominant factor leading to a decrease in the overall dielectric constant. © *2001 American Institute of Physics.*
[DOI: 10.1063/1.1388861]

I. INTRODUCTION

As the design rule of integrated circuit (IC) devices approaches 0.1 μm and beyond, the interconnection delay (RC delay) begins to govern overall device delays. In addition, the shrinkage of device dimensions causes cross talk between signal paths and higher power consumption. To realize high performance in IC devices it is necessary to reduce the RC delay, cross talk, and power consumption. An effective method to make these reductions is to decrease the parasitic capacitance by employing a low dielectric constant (low-k) material in the intermetal dielectrics (IMD).[1,2] Over the past few years, fluorinated SiO_2 (SiOF)[3] films and hydrogen silsesquioxane (HSQ) have been studied for this application, but it has been reported that they are limited to reducing the dielectric constant below 3.0.[2,4]

Recently, various organic polymers and carbon-based composite materials were extensively investigated for low-k IMD materials as an alternative to conventional SiO_2. Among the materials investigated, carbon-incorporated silicon oxide (SiOC) is considered a promising candidate in the 0.13 μm technology and beyond.[5] Previously we reported that it is possible to reduce the dielectric constant of a SiOC film to 2.4 and that the film is thermally stable up to 500 °C.[6] Korczynski[7] and Pang[8] reported that the low dielectric constant of a SiOC film resulted from hydrocarbon (methyl group, $-CH_3$) incorporation and the film's low density. However, the exact mechanism to reduce the dielectric constant of SiOC films has not been clearly understood until now.

In this study the origin of the low dielectric constant of SiOC films was investigated by examining the dielectric contribution of electronic, ionic, and dipolar polarization. Each contribution of these polarization modes was also investigated in thermally grown silicon dioxide (thermal oxide) and silicon oxide deposited by plasma enhanced chemical vapor deposition (PECVD) while using a tetraethoxysilane precursor (PE-TEOS oxide) for comparison.

II. EXPERIMENT

A. Thin film preparation and characterization

SiOC films were deposited on p-type (100) Si substrates by PECVD using a bis-trimethylsilylmethane (BTMSM) liquid precursor. The PECVD system used in this study and the detailed deposition conditions have been described elsewhere.[6] Thermal oxides were grown by dry oxidation of

a)Electronic mail: hjkim@plaza.snu.ac.kr

the Si substrate at 1 atm and O_2/N_2 ambient conditions. The tetraethoxysilane precursor (PE-TEOS) oxide films were deposited by PECVD using a tetraethoxysilane (TEOS) precursor. The film thickness and refractive index were measured by ellipsometry, at a wavelength of 632.8 nm (model: Gaertner L116-HP85B) and spectroscopic ellipsometry (model: Sopra ESVG). The chemical bonding state and the dielectric constant in the IR region of the SiOC film were characterized by using Fourier transform infrared (FTIR) spectroscopy. This was operated in the absorbance and reflectance mode with a Bio-Rad FTS40. The film composition was determined by elastic recoil detection time-of-flight (ERD-TOF) analysis. The film density was directly calculated from the ratio of mass to volume of the film. The film mass was measured by an electronic balance (model: AND HM202) with a resolution of 0.01 mg. The film volume was calculated by three-dimensional mapping of the film thickness, measured at 625 different points on the 4-in. wafer. The dielectric constant at 1 MHz was obtained by a HP4280A $C-V$ meter on the metal–insulator–semiconductor (MIS) structure.

B. Analysis of dielectric polarizations

The dielectric constant is a frequency-dependent, intrinsic material property. The constant can be divided into three components that result from electronic, ionic, and dipolar polarization. The dielectric constants measured at 1 MHz consist of electronic ($\Delta\varepsilon_e$), ionic ($\Delta\varepsilon_i$), and dipolar ($\Delta\varepsilon_d$) contributions, as expressed in

$$\varepsilon_r(\text{at } 1 \text{ MHz}) = 1 + \Delta\varepsilon_e + \Delta\varepsilon_i + \Delta\varepsilon_d. \tag{1}$$

The dielectric constant of a material can also be calculated from the refractive index, as expressed in

$$\varepsilon_r(\lambda) = n^2(\lambda) + k^2(\lambda), \tag{2}$$

where ε_r is a relative dielectric constant, n is a real part of a refractive index, k is an imaginary part of a refractive index, and λ is the wavelength of a light source.

The pure electronic contribution to the dielectric constant ($\Delta\varepsilon_e$) was calculated from the refractive index obtained in the visible-ultraviolet (vis-UV) region. Since the extinction coefficient k of SiO_2-based materials is normally negligible in this region, the relative dielectric constant in Eq. (2) can be simply expressed as n^2.[9,10]

The ionic contribution to the dielectric constant ($\Delta\varepsilon_i$) was calculated by subtracting the dielectric constant at 632.8 nm, $1+\Delta\varepsilon_e$, from the dielectric constant in the IR region, $1+\Delta\varepsilon_i+\Delta\varepsilon_e$. To obtain the dielectric constant in the IR region, the refractive index was calculated from the Kramers–Kronig dispersion relation.

The original Kramers–Kronig relation is expressed as in[10–13]

$$n_i = 1 + \frac{\pi}{2} P \int_0^{\infty} \frac{\nu k(\nu)}{\nu^2 - \nu_i^2} d\nu, \tag{3}$$

where n_i is the real part of the refractive index at the ith wave number, P is the principal value ensuring integral from zero to infinity, ν_i is a wave number at i, and k is the imaginary part of the refractive index (extinction coefficient).

The integration in Eq. (3) cannot be performed from zero to infinity since the IR spectrum is obtained only in a finite region (650–4000 cm^{-1}). By introducing the refractive index at 632.8 nm (n_e, ν=15 800 cm^{-1}), the above integration is approximated in a finite region of the IR spectrum as is shown in Eq. (4). The dielectric constant in the range from 4000 cm^{-1} to infinity is approximated as the dielectric constant at 632.8 nm calculated from the refractive index by ellipsometry, as explained in Eq. (2).

$$n_i \cong n_e + \frac{\pi}{2}\left[\int_{650}^{\nu_i} \frac{\nu k(\nu)}{\nu^2 - \nu_i^2} d\nu - \int_{\nu_i}^{4000} \frac{\nu k(\nu)}{\nu^2 - 15\,800^2} d\nu\right], \tag{4}$$

where n_e is the refractive index at 632.8 nm (15 800 cm^{-1}).

The IR reflectance spectra of the films were obtained from FTIR spectroscopy (Bio-Rad FTS40). The commercial program WIN-IR™ (from Bio-Rad) was used to transform these reflectance spectra into IR region refractive indices. The IR region dielectric constants were calculated by Eqs. (2) and (4). However, the ionic contribution obtained from this transformation may not be quantitatively precise due to some approximations used in the transformation calculation and the restricted instrumental resolution of FTIR spectroscopy. To manage this lack of precision the IR region dielectric constants were corrected by normalizing with the thermal oxide ionic contribution ($\Delta\varepsilon_i$). The thermal oxide value $\Delta\varepsilon_i$ was obtained from Eq. (1), where $\Delta\varepsilon_d$ is zero, $(1+\Delta\varepsilon_e)$ is the same as the square of the refractive index at 632.8 nm, and ε_r is obtained from the $C-V$ measurement at 1 MHz.

The dipolar polarization was qualitatively estimated by the Clausius–Mosotti relation in[9,14]

$$\left[\frac{(\varepsilon_r - 1)}{(\varepsilon_r + 2)}\right] = \frac{\rho}{M} \times \frac{N_A}{3\varepsilon_0}(\alpha_{ie} + \alpha_d),$$
$$\alpha_d = \frac{p^2}{3kT}(\text{dipolar polarizability}), \tag{5}$$

where M is molecular weight, ρ is density, ε_r is the dielectric constant at 1 MHz, ε_0 is the vacuum dielectric constant, α_{ie} is the electronic and ionic polarizability, α_d is the dipolar polarizability, p is the dipole moment, k is the Boltzmann constant, and T is absolute temperature.

Unlike electronic and ionic polarizabilities, dipolar polarizability is inversely proportional to temperature, as is shown by Eq. (5). Therefore the temperature dependence of the polarizability per unit volume can imply that a dipole moment exists in the film. In this study, this dependence was investigated by varying the measurement temperature from 20 to 180 °C.

III. RESULTS AND DISCUSSION

Thermal oxide film was grown in a dry oxidation atmosphere at 1000 °C. PE-TEOS oxide and SiOC films were deposited on p-type Si(100) by PECVD. The carbon content incorporated into the films was controlled by the substrate temperature. The basic physical properties of the films are summarized in Table I.

TABLE I. Physical properties of thermal oxide, PE-TEOS oxide, and SiOC films having varying carbon content.

	Thermal oxide	PE-TEOS oxide	SiOC		
			low	mid	high
film thickness (nm)	105.4	103.8	100.0	100.0	99.8
refractive index (at 632.8 nm)	1.458	1.462	1.435	1.396	1.360
film density (g/cm^3)	2.40	2.24	2.09	1.59	1.17
porosity (%)[a]	0	NA	13.6	23.6	39.0
carbon content (at. %)[b]	NA	NA	5.5	10.5	19.6
[chemical composition]			[$SiO_{1.9}C_{0.17}$]	[$SiO_{1.3}C_{0.27}$]	[$SiO_{0.9}C_{0.46}$]

[a]Porosity (%) was calculated from the film density and molar weight of each composition, based on the assumption that the thermal oxide has no porosity.
[b]at. % (from ERD-TOF)=100×[C]/([Si]+[O]+[C]).

Figure 1 shows the variation of film densities and refractive indices measured at 632.8 nm as a function of film carbon content. The refractive index of the PE-TEOS oxide film was slightly higher than that of the thermal oxide film. This difference is due to the two films' composition differences. As more carbon was incorporated into the SiOC film, both the film density and refractive index decreased. Previously, we reported that the decrease of film density in SiOC films resulted from termination of the O–Si–O bonding network by replacing oxygen atoms with hydrocarbon groups ($-CH_n$).[6] The SiOC film density was reduced to half the value of the PE-TEOS oxide density when the carbon content was increased to 19.6 at. %, while the refractive index slowly decreased from 1.46 to 1.36. For "aerogel" and "xerogel," which are low dielectric constant materials having the same composition as PE-TEOS oxide of SiO_{2-x}, their refractive indices are about 1.20 when their film densities are half that of the PE-TEOS oxide.[15] Considering that the incorporation of hydrocarbon groups ($-CH_n$) altered the SiOC film stoichiometry, as shown in Table I, the relatively small refractive index decrease was attributed to the change of SiOC film's molar electronic polarizability. This change resulted from the compositional change.

The dielectric constants measured at 1 MHz and the electronic dielectric constants obtained from the squares of the refractive indices at 632.8 nm are shown in Fig. 2. The dielectric constants at 1 MHz declined drastically with increased carbon content of the SiOC film. The decrease of the electronic contribution ($\Delta\varepsilon_e$) to the dielectric constant was quite small in comparison with the variation of the dielectric constant at 1 MHz. From these results we found that either ionic ($\Delta\varepsilon_i$) or dipolar ($\Delta\varepsilon_d$) contributions to the dielectric constant were the dominant factors to reduce the dielectric constant of the SiOC film, rather than that from the electronic contribution ($\Delta\varepsilon_e$). However, there is no information on the separate values of each $\Delta\varepsilon_i$ or $\Delta\varepsilon_d$, as only their combined contribution to the dielectric constant measured at 1 MHz is available.

To examine the amount of ionic contribution to the SiOC film's dielectric constant we calculated the dielectric constants in the IR region. This was calculated from the IR reflectance spectra by using the Kramers–Kronig transformation method described in the previous section. Figure 3 represents the dispersive characteristics of the dielectric constants in the IR region of 650–4000 cm^{-1}. When the wavelength of the applied IR light exceeds about 1300 cm^{-1}, the ionic polarization can no longer follow the applied field and thus the dielectric constant is only composed of the electronic contribution ($1+\Delta\varepsilon_e$). In the region of 1000–1300 cm^{-1}, a resonant increase of the dielectric constant occurs

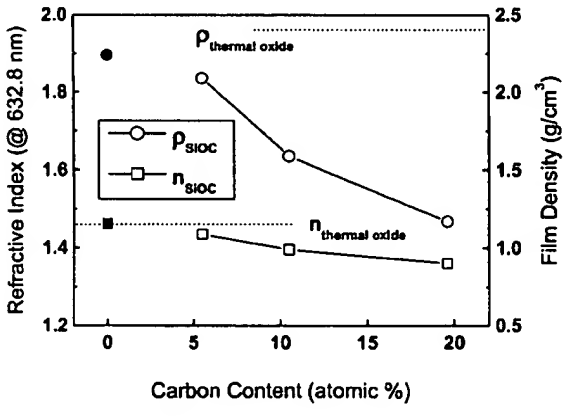

FIG. 1. Variations of film density and refractive index for the PE-TEOS film and the SiOC films as a function of carbon content.

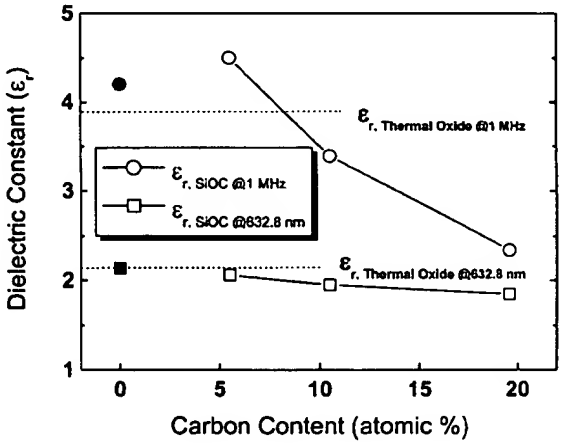

FIG. 2. Variations of dielectric constants, measured at 1 MHz, and electronic dielectric constants, calculated from the refractive index at 632.8 nm, for the PE-TEOS film, and the SiOC films as a function of carbon content.

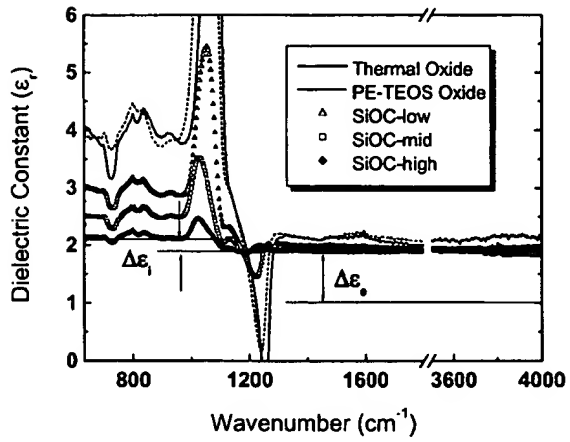

FIG. 3. Dielectric constants in the IR region calculated from the IR reflection spectra for the thermal oxide, PE-TEOS oxide, and SiOC films by using the Kramers–Kronig relationship. Magnitude of the dielectric constants was corrected by normalizing with the ionic contribution ($\Delta\varepsilon_i$) of the thermal oxide (1.80).

due to IR absorbance by the Si–O stretching vibration mode (near 1100 cm^{-1}) in the SiOC film. The ionic contributions, due to other vibration modes in the SiOC film, are negligible because IR absorbances by other modes are considerably smaller than that by the Si–O stretching mode.[10,16] At lower than the resonant frequency in the IR region, the dielectric constant contains the ionic contribution ($\Delta\varepsilon_i$) as well as the electronic contribution.

As more carbon was incorporated in the SiOC films, the ionic contribution ($\Delta\varepsilon_i$) to the dielectric constant decreased gradually, as depicted in Fig. 3. The reduced ionic contribution might be a consequence of a decrease of the Si–O bond in the film, which has strong ionic polarization.[9,10] A previous study has shown that the Si–CH_n bond terminated the O–Si–O bonding network, causing a decrease in film density.[6] We note that the ionic contribution's decrease can be explained by a decrease in film density. The replacement of Si–O by Si–CH_n bonds can also play a role in decreasing the ionic contribution due to the Si–CH_n bond being less ionic than the Si–O bond. With increasing degree of replacement, the oxygen deficiency in the film markedly increased, as shown in Table I. This led to a decrease of the ionic contribution due to the additional reduction of the Si–O bond. Thus we can conclude that the decrease of Si–O bonds played a crucial role in reducing the measured ionic contribution to the dielectric constant. As is shown in Fig. 3, the lower intensity of the resonant peak (near 1100 cm^{-1}), for a film having higher carbon content, corresponds to a lower ionic contribution. This is good verification of our deductions.

Using Eq. (1), each contribution to the dielectric constant can be calculated from the dielectric constant measured at 1 MHz (ε_r), the refractive index (n), and the ionic contribution ($\Delta\varepsilon_i$) of Fig. 3. Electronic, ionic, and dipolar contributions ($\Delta\varepsilon_e$, $\Delta\varepsilon_i$, and $\Delta\varepsilon_d$) to the dielectric constant, with respect to the film carbon content, are summarized in Table II. The value of $\Delta\varepsilon_d$ was obtained by subtraction of ($n^2+\Delta\varepsilon_i$) from ε_r. It should be noted that $\Delta\varepsilon_i$ and $\Delta\varepsilon_d$ are not exact values but are normalized values from $\Delta\varepsilon_i$ (1.80) of the thermal oxide. This is based on the assumption that the thermal oxide has no dipolar polarization.

As mentioned above, the electronic contribution in the SiOC films was slightly decreased with increasing carbon content, but carbon content had little influence on reducing ε_r. On the other hand, the ionic contribution drastically decreased as more carbon was incorporated. This decrease in the ionic contribution is a predominant factor for the low dielectric constant of the SiOC films. However, the SiOC films showed considerable dipolar contributions when contrasted with the thermal oxide and PE-TEOS oxide. Since a [SiO_4] tetrahedron is symmetric, pure silicon dioxide does not have a dipolar polarization. When a hydrocarbon group ($-CH_n$) replaces an oxygen site, the [SiO_4] tetrahedron loses its symmetry by changing into [$SiO_3(CH_n)$]. The carbon incorporation, moreover, led to the oxygen-deficient SiOC film, as summarized in Table I. These configurational changes help explain the increased dipolar contribution in the SiOC films. Interestingly, even though carbon incorporation promotes dipole generation, the dipolar contribution of a film having a higher carbon content was lessened. This result can be explained by considering the film density. The SiOC film with a higher carbon content has a larger molar dipole moment than that with lower carbon content; nevertheless, its smaller density is considered to cause the reduction of apparent dipolar contribution.

Considering the Clausius–Mossotti relation [Eq. (5)], the dipolar contribution ($\Delta\varepsilon_d$) could be qualitatively esti-

TABLE II. Dielectric constants in various frequency regions and contribution values for thermal oxide, PE-TEOS oxide, and the SiOC films having varying carbon content.

	Thermal oxide	PE-TEOS oxide	SiOC		
			low	mid	high
$1+\Delta\varepsilon_e$[a]	2.13	2.14	1.97	1.96	1.90
$1+\Delta\varepsilon_e+\Delta\varepsilon_i$[b]	3.90	3.97	2.96	2.52	2.15
$1+\Delta\varepsilon_e+\Delta\varepsilon_i+\Delta\varepsilon_d$[c]	3.90	4.20	4.50	3.39	2.34
$\Delta\varepsilon_e$	1.13	1.14	0.97	0.96	0.90
$\Delta\varepsilon_i$	1.77	1.83	0.99	0.56	0.25
$\Delta\varepsilon_d$	0	0.23	1.54	0.87	0.19

[a]$(1+\Delta\varepsilon_e)$ is obtained from n^2 (at 632.8 nm).
[b]$(1+\Delta\varepsilon_e+\Delta\varepsilon_i)$ is obtained from Kramers–Kronig conversion of the IR reflection spectrum.
[c]$(1+\Delta\varepsilon_e+\Delta\varepsilon_i+\Delta\varepsilon_d)$ is obtained from $C-V$ measurement at 1 MHz.

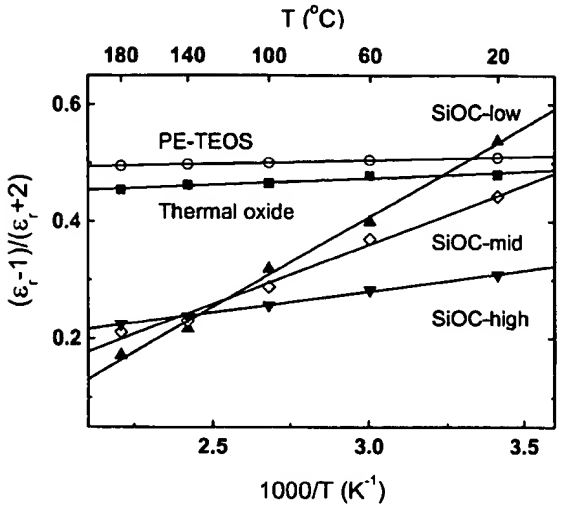

FIG. 4. Variations of the polarizability per unit volume for the thermal oxide, PE-TEOS oxide, and SiOC films as a function of measurement temperature.

mated from the temperature dependence of the polarizability per unit volume $[(\varepsilon_r-1)/(\varepsilon_r+2)]$. The variation of the dielectric constant (ε_r) due to measurement temperature and carbon content in the film was determined. Figure 4 shows the variation in the polarizability as a function of the temperature used in the $C-V$ measurements at 1 MHz. The measured polarizability of the SiOC film was inversely proportional to the temperature and its slope to $(1/T)$, which is proportional to the dipole moment per unit volume, and was gradually reduced with increasing carbon content of the film. Both the thermal oxide and PE-TEOS oxide films showed very little temperature dependence of their polarizablity and from this the negligible dipolar contribution in each film[10,16] could be confirmed. These results are in good agreement with the dipolar contribution values shown in Table II.

IV. CONCLUSION

The electronic, ionic, and dipolar contributions to the dielectric constants of the SiOC films were separately investigated using their frequency-dependent dielectric constants. The electronic contribution slightly decreased with increasing carbon content. This reduction of the electronic contribution can be explained by a decrease in the film density. However, the reduced electronic contribution had little influence on reducing the overall dielectric constant. The ionic contribution significantly decreased as more carbon was incorporated. This appears to be caused by decreased film density, replacement of Si–O by $Si-CH_n$, and increased oxygen deficiency of the film. On the contrary, the SiOC films showed considerable dipolar contributions as compared with the thermal oxide and PE-TEOS oxide. This dipolar contribution is considered to result from a configurational change of $[SiO_4]$ tetrahedron due to carbon incorporation. However, the film having a high carbon content showed a negligible dipolar contribution as the decreased film density contributed to reducing the dipole concentration. Therefore the low dielectric constant of the SiOC films mainly results from reduction of the ionic contribution, which can be explained by the decrease of the Si–O bond in the film.

ACKNOWLEDGMENTS

The authors acknowledge the financial assistance for this work by the Jusung Engineering Co. The authors sincerely thank Dr. K. Krishnan at Bio-Rad Lab. for analyzing the IR reflectance using his software and his helpful advice about the Kramers–Kronig transformation. The authors also thank S. W. Lee at Samsung Electronics for his efforts in SE analysis.

[1] T. Homma, Mater. Sci. Eng., R. **23**, 243 (1998).
[2] C. H. Ting and T. E. Seidel, Mater. Res. Soc. Symp. Proc. **381**, 3 (1995).
[3] Y.-H. Kim, H.-H. Kim, S.-K. Lee, H. J. Kim, S.-O. Kim, and Y.-S. Son, J. Korean Phys. Soc. **33**, S179 (1998).
[4] L. Peters, Semicond. Int. **21**, 64 (1998).
[5] L. Peters, Semicond. Int. **23**, 108 (2000).
[6] Y.-H. Kim, S.-K. Lee, and H. J. Kim, J. Vac. Sci. Technol. A **18**, 1216 (2000).
[7] E. Horczynski, Solid State Technol. **42**, 43 (1999).
[8] B. Pang, W.-F. Yau, P. Lee, and M. Naik, Semicond. Fabtech **10**, 7 (1999).
[9] W. D. Kingery, H. K. Bowen, and D. R. Uhlmann, *Introduction to Ceramics* (Wiley, New York, 1976).
[10] S. M. Han and E. S. Aydil, J. Appl. Phys. **83**, 2172 (1998).
[11] M. I. Strashnikova and E. V. Mozdor, J. Exp. Theor. Phys. **87**, 756 (1998).
[12] H. A. Kramers, Atti Congr. Int. Fis. Como **2**, 545 (1927).
[13] E. de L. Kronig, J. Opt. Soc. Am. **12**, 547 (1926); Rev. Sci. Instrum. **12**, 547 (1926).
[14] M. A. Omar, *Elementary Solid State Physics* (Addison-Wesley, New York, 1975).
[15] S. V. Nitta, V. Pisupatti, A. Jain, P. C. Wayner, W. N. Gill, and J. L. Plawsky, J. Vac. Sci. Technol. B **17**, 205 (1999).
[16] S. W. Lim, Y. Shimogaki, Y. Nakano, K. Tada, and H. Komiyama, Jpn. J. Appl. Phys., Part 1 **35**, 1468 (1996).

Exhibit E 09/912,737

Building Copperopolis II

Using optical metrology to monitor low-k dielectric thin films

Feng Yang and William A. McGahan, *Nanometrics;* and Carol E. Mohler and Lisa M. Booms, *Dow Chemical*

Because controlling curing temperature and time is critical for producing high-quality spin-on dielectr thin films, rapid feedback from metrology tests on thermal process tools is needed to correct tool drift.

As device features of ULSI circuits continue to shrink, the capacitance of the interlevel dielectric (ILD) material becomes an increasingly limiting factor on the overall performance of these chips. An industrywi effort is under way to search for a next-generation low-k ILD material to replace traditional silicon dioxid Many potential low-k materials belong either to the inorganic polymer family (e.g., organosilicates) or the organic polymer family.[1,2] The molecular structure of the cross-link network in these polymers is critical because it affects their electrical, thermal, and mechanical properties as well as their optical properties, suc as index of refraction (n) and extinction coefficient (k). Because n and k values depend both on the electronic structure of a polymer and on its porosity, they can serve as good indicators for monitoring low polymer formation.

One low-k ILD material is SiLK from Dow Chemical (Midland, MI), a spin-on organic polymer that can b readily deposited using a conventional spin-coater. This dielectric thin film in its as-deposited state must undergo a thermal curing process to form a desired polymer structure and to achieve correct mechanical, thermal, and electrical properties. The curing process takes place at temperatures between 400° and 450°C in standard thermal-processing equipment (furnaces, ovens, or hot-plates). The cured resins have a dielectr constant of 2.65 and can withstand temperatures as high as 490°C. Their high thermal stability permits integration with current multilevel interconnect processes. However, because the polymerization of these resins is thermally activated, controlling the curing temperature and time is critical to producing high-quality cured films.[3,4] Thus, it is essential to have immediate feedback from metrology tests on thermal process tools to detect and correct tool drift promptly. This article discusses optical metrology methods fo monitoring cured low-k dielectric thin films.

Thin-Film Optical Metrology

One of the most important advantages of optical metrology arises from its nondestructive nature, which permits measurements on product wafers and active device areas. In-line optical metrology can monitor th performance of thermal processing equipment by conducting real-time measurements on product wafers, thus eliminating monitor wafers and minimizing rework or loss of product wafers as a result of out-of-control equipment.

Thin-film optical metrology provides fast and precise real-time measurements of thin-film thicknesses and optical constants. In semiconductor manufacturing, spectroscopic reflectometry and ellipsometry are wide

used optical metrology methods for measuring these parameters in-line. Thin-film metrology tools measu the reflectance or ellipsometric spectrum of thin films and extract values of thicknesses or optical constant

Because there are a maximum of two independent optical measurement data (Ψ and Δin spectroscopic ellipsometry) at each wavelength (λ), the maximum number of unknowns that can be determined in the whole spectrum is $2W$ (where W is the number of wavelengths). Materials with finite light absorption hav two unknowns (n and k) at each wavelength and one additional unknown in the film thickness. Therefore, the total number of unknowns is double the number of wavelengths plus one--that is, $2W + 1$. Because the number of unknowns resulting from $2W + 1$ is at least one too many to be determined from available spectroscopic ellipsometry or spectroscopic reflectometry data, it is necessary to employ a dispersion mod which describes the functional dependence of n's and k's on wavelength based on N fit parameters. Therefore, the total number of unknowns becomes $N + 1$. As long as $2W \geq N + 1$, film thickness and optica constants can be determined simultaneously by numerically iterating $N + 1$ variables to fit spectra.

The results of the research discussed in this article on the use of optical metrology to monitor a low-k resi curing process demonstrate that with a correct dispersion model, the n(λ), k(λ), and thickness values for a dielectric thin film can be determined from reflectance measurements. In the ultraviolet (UV) spectral region, the refractive indices values (RIs), or n(λ)s, are found to correlate to the curing conditions. By measuring the variation of n, the degree of curing in the resin can be monitored. For example, at a wavelength of 314 nm, the RIs of dielectric thin films change systematically with the curing parameters o temperature and time.

Based on the relationship between the optical constants of resins and their curing parameters, a single-parameter empirical interpolation model for resin optical constants was developed. With this interpolation model, the curing of the resins can be readily monitored with an automated thin-film optical metrology to that provides prompt feedback on the condition of the thermal processing equipment.

Sample Preparation and Instrumentation

For this study, a matrix of SiLK-I dielectric thin-film samples was prepared by varying the curing temperature and time. First, a spin-on process deposited resins on bare silicon wafers, which then went through a hard bake step at 310°C for 90 seconds and were subsequently cured on hot plates in a nitrogen ambient. The curing temperature varied from 400° to 470°C and the curing time from 30 to 360 seconds. The sample thicknesses were approximately 7400 Å.

To determine the optical constants n(λ) and k(λ) of these samples, a variable-angle spectroscopic ellipsometer (VASE) from J. A. Woollam (Lincoln, NE) was used.[5] A very powerful off-line analysis instrument for the characterization of the optical properties of thin films, this instrument utilizes a monochrometer to control incident light wavelength so that only the light of a single wavelength is incide onto the sample during each measurement.[6] It measures two ellipsometric data at each wavelength, $\Psi$and and completes the spectrum by scanning through all wavelengths. This way, the measured $\Psi$and Δspectra truly represent the spectroscopic response of the sample. If a thin film's thickness is known, its n (λ) and k(λ) can be accurately determined by direct calculation from $\Psi$and Δvalues.

In general, organic polymers are transparent or nearly transparent in the visible spectral region, from whic their thicknesses can be extracted by fitting that part of a spectrum using a Cauchy dispersion formula. Th

complicated optical constant response in the UV spectral region can then be determined directly from Ψan Δspectra.[7] By choosing an appropriate dispersion model for the optical constants, the complicated n and k spectra from the VASE measurement results were parameterized. The production worthiness of the parametric dispersion model was tested by running it on a NanoSpec 8000XSE high-throughput thin-film metrology tool from Nanometrics (Sunnyvale, CA). This tool determines thickness values and the n's and of thin films by measuring and fitting spectroscopic reflectance spectra, spectroscopic ellipsometric spectr or a combination of both. Its modeling capability and data-fitting algorithm enable the analysis of data fro a wide range of materials and layered structures while simultaneously determining thickness and optical constants.[8]

Single-Parameter Empirical Interpolation

Using the VASE measurements, a spectral window between 280 and 340 nm was found where the RIs of the thin-film samples changed monotonically with cure temperature and time. Figure 1 shows the measurements for UV spectra only. In the visible-wavelength region, RI variation was not significant. As demonstrated in both Figures 1a and 1b, sensitivity to the curing parameters of time and temperature was highest at a wavelength of 314 nm. The total magnitude of the RI change was 0.065 at this wavelength. Figure 2 plots RI for all test samples at 314 nm, denoted as n(314 nm). Since the n(314 nm) value decreas when either the curing time or temperature was increased, the n(314 nm) variation can serve as an indicatc of the degree of curing in the dielectric thin film. The reduction in the n(314 nm) value decreased as the temperature or time approached the high end of the curing process window, indicating that the curing process was nearly completed. After determining the correlation between curing parameters and optical constants, a single-parameter empirical interpolation model could be employed.

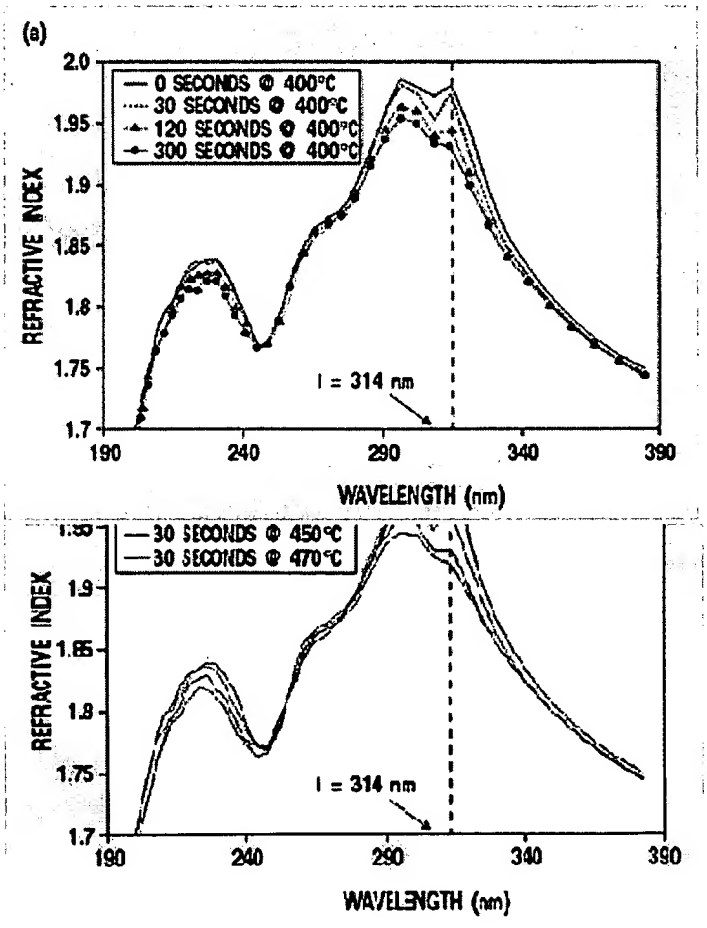

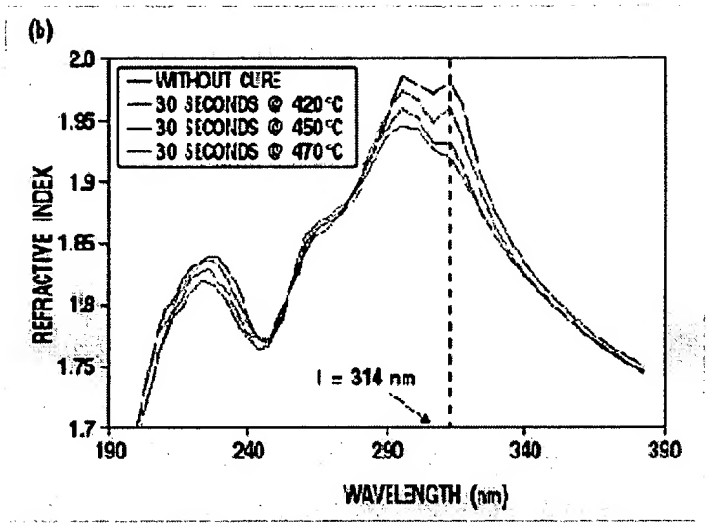

Figure 1: VASE measurements of the ultraviolet RIs of low-k resins cured under different conditions: (a) cure-time dependence; (b) cure-temperature dependence.

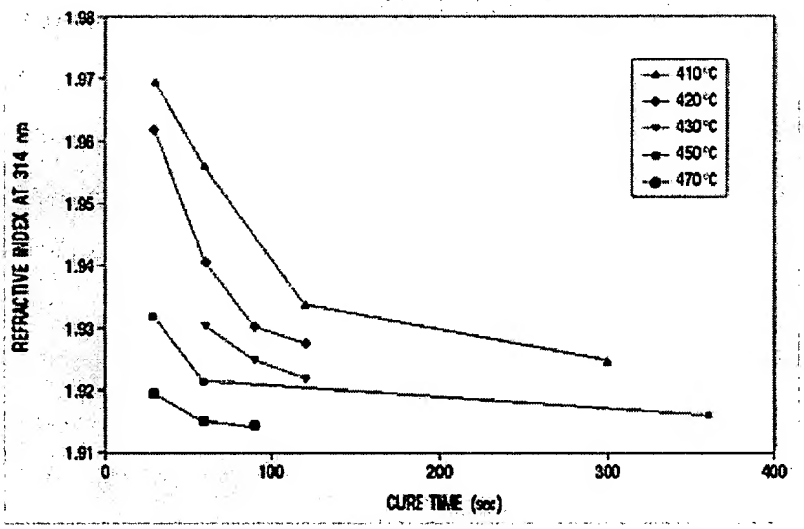

Figure 2: VASE measurements of RIs at 314 nm at different curing times and temperatures.

In a process-sensitive thin film, process parameter variations can lead to changes in the film's n(λ) and k(. values. That is the case for the cured resins investigated in this study. Monitoring the degree of curing in these dielectric thin films on an automated metrology tool requires a parametric dispersion model for the optical constants of these resins, which represents the functional dependence of n(λ) and k(λ) on λ in tern of a small number of adjustable parameters. This model should be able to describe the n(λ) and k(λ) of these resins cured under all conditions within the whole process window.

An empirical interpolation model is an effective single-parameter dispersion model whose adjustable parameter normally corresponds to a process-dependent physical property (e.g., the crystallinity of polysilicon or the alloy fraction ratio of SiGe).[9] It consists of a database of optical constant spectra for a given material. Each spectrum corresponds to a specific process condition. When fitting reflectance or

ellipsometry data of a sample prepared under unknown conditions (within the process window), the sampl optical constants are interpolated between known spectra in the database. With only one adjustable parameter, the correlation between thickness and optical constants can be minimized during data analysis.

To develop an empirical interpolation model for these low-k resins, optical constant spectra of five sample cured under different conditions were chosen. The n(314 nm) values of these samples, which are presentec in Table I, were evenly distributed between the lowest and highest values in the process window. The term *cure index* was used to refer to the adjustable parameter in the model. A cure index value of 0 was assigne to the uncured sample, which had the highest n(314 nm) value, while an index of 1 was assigned to the cured sample with the lowest n(314 nm) value. The other three cured samples were evenly spaced betweer the samples with the highest and lowest n(314 nm) values. The cure indices were determined by proportioning the n(314 nm) values of the five samples between 0 and 1 as follows:

$$\text{Cure index} = [n(314\text{ nm}) - 1.9791]/[1.9161-1.9791]$$

Automated Production Metrology

The empirical interpolation model for low-k resins was tested on the automated thin-film metrology tool. Using the tool's reflectometer mode, both film thickness and optical constants were determined from a recipe set up to measure absolute UV-visible reflectance.[10] Figure 3, which presents a reflectance scan-anc fit result based on the empirical interpolation model, shows an excellent match between the experiment an the model. To become production worthy, however, the metrology method must demonstrate high levels c precision, stability, accuracy, sensitivity, and throughput.

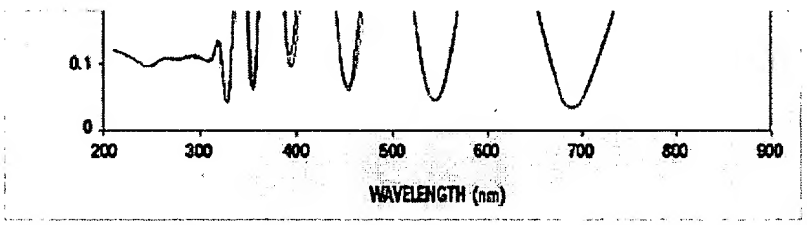

Figure 3: Fit result of reflectance data from low-k resin treated at 400°C for 300 seconds shows an excellent match between the experiment and the model.

Sample	Cure	n(314nm)	Cure

No.	Condition		Index
1	Without cure	1.9791	0.00
2	30 seconds @ 410°C	1.9694	0.15
3	60 seconds @ 400°C	1.9513	0.44
4	60 seconds @ 430°C	1.9307	0.77
5	360 seconds @ 450°C	1.9161	1.00

Table I: Data for five samples whose optical constant spectra made up the single-parameter interpolation model.

The measurement precision and dynamic stability of the metrology tool were tested by examining several wafer samples that had varying film thicknesses or had been cured under different conditions. One of the worst cases was a 1000-Å-thick resin sample that was loaded 10 times and measured in five places at each load (one at the center and four around the edge). The results revealed that the standard deviation of n(314 nm) for 10 loads at each site was <0.001 and that the variation of the average value of n(314 nm) for five sites was also <0.001 from load to load. Since the uncertainty was <2% of the total range of the variation i n(314 nm) that may be induced by curing (about 0.063), it was concluded that this measurement technique provides sufficient precision and stability to monitor the curing process of these low-k resins. Table II lists the statistical results of the average thickness and n(314 nm) of each load.

	Mean	Standard Deviation
Thickness (Å)	1064.8	1.14
n(314 nm)	1.929	<0.001

Table II: Statistical test results from a worst-case 1000-Å-thick sample that was loaded 10 times and measured at five places after each load.

By comparing n(314 nm) values measured by the automated in-line tool to the benchmark values from the VASE measurement, measurement accuracy could be evaluated. Figure 4 shows that the data points fit a straight line with a slope of 0.9788 and a y-intercept of 0.0441, indicating excellent correlation between th two types of measurements. This close match demonstrates that the refractive index measurements using t reflectometry mode of the in-line tool were accurate for monitoring the curing process.

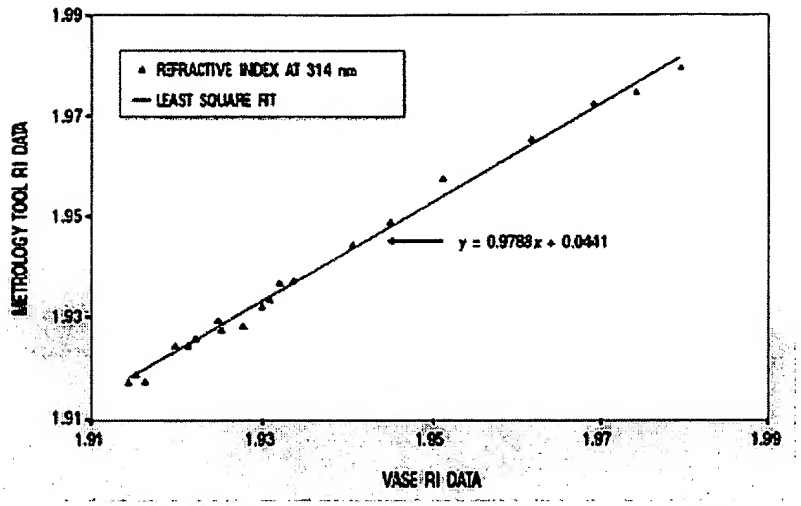

Figure 4: Correlation between RI at 314 nm measured by the VASE and the automated metrology tool shows an excellent match between the two types of measurements.

The model's sensitivity to the curing process as well as the feasibility of determining the film thickness an optical constants simultaneously are seen in Figure 5, which plots three model-predicted reflectance specti corresponding to three cure conditions: 30 seconds at 410°C, 30 seconds at 420°C, and 60 seconds at 420° All three spectra were generated based on the same thickness value of 7400 Å. The difference between the spectra is strictly a result of the difference in the degree of cure. Figure 5 clearly demonstrates that there is significant difference among these spectra in the UV spectral region (between 310 and 400 nm), which cai be readily measured by a reflectometer. Film thickness information, on the other hand, can be found in the period of the oscillating portion of the reflectance spectrum. By fitting a broadband UV-visible reflectance spectrum, film thickness can be measured quickly and reliably, and the cure-induced change in the resins can be monitored.

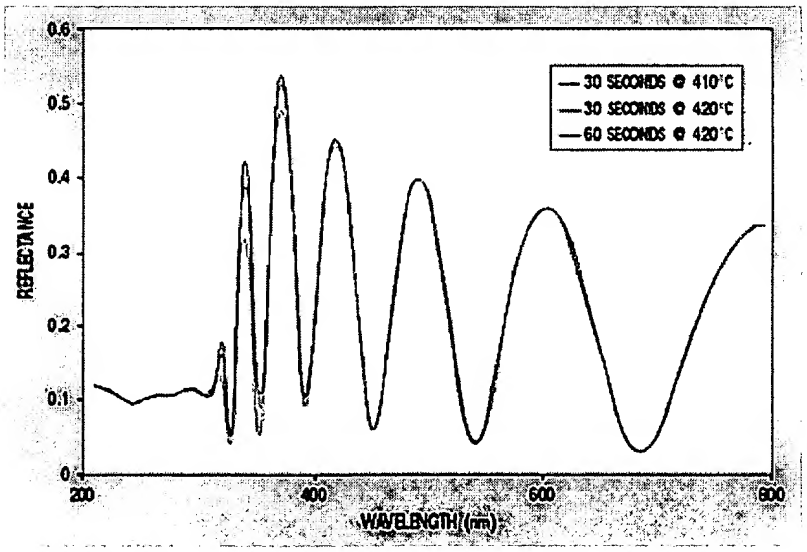

Figure 5: Reflectance sensitivity predicted by the empirical interpolation model for low-k resins under

three different cure conditions; the difference between the spectra is a result of the difference in the degre of cure.

Measurement throughput depends on the speed of reflectometer data acquisition and analysis, as well as th focusing speed of the sample stage (e.g., the system's robotics). To boost the UV signal-to-noise ratio, a broadband measurement requires longer detector integration time than a visible reflectance measurement, leading to decreased throughput. The metrology tool used in this study performed measurements at five sit on an 8-in. wafer in approximately 1 minute with focusing on each site. New-generation spectrophotomete heads, robotics, and data-handling software are in the final testing stages, promising much improvement in measurement throughput.

Conclusion

In order to serve as adequate low-k ILD materials, organic spin-on polymers must be properly cured. In-lin characterization of the curing process is crucial because it improves equipment efficiency, eliminates the need for monitor wafers, and reduces wafer scrap and wasted work. The curing process of low-k resins can be monitored with broadband reflectometry, and film thickness and the degree of curing can be calculated simultaneously. Because of its fine measurement spot size and pattern recognition capability, this technique can be used to monitor the curing process of low-k thin films on product wafers. The method described here for monitoring SiLK should be applicable to other low-k materials if the change in the optical constants induced by polymerization is monotonically related to the process parameter and the metrology tool is sensitive enough to measure the change in optical constants. Additonal studies must be performed to determine the feasibility of performing metrology measurements on product wafers with device structures and the efficacy of using integrated in-line metrology tools.

Acknowledgment

Portions of the material covered in this article were first presented at the Advanced Metallization Conference in Orlando, FL, September 28–30, 1999.

References

1. NH Hendricks, "The Status of Low-k Materials Development," in *Proceedings of the Sixth International Dielectrics for ULSI Multilevel Interconnection Conference* (Tampa, FL: IMIC, 200(17–26.
2. W Volksen et al., "Characterization of Porous Organosilicates for On-Chip Applications," in *Proceedings of the Sixth International Dielectrics for ULSI Multilevel Interconnection Conference* (Tampa, FL: IMIC, 2000), 67–76.
3. PH Townsend et al., "SiLK Polymer Coating with Low Dielectric Constant and High Thermal Stability for ULSI Interlayer Dielectric," in *Proceedings of the Materials Research Society* 476 (Warrendale, PA: Materials Research Society, 1997), 9–17.
4. S Allada, "Low K Adhesion Issues in Cu/Low K Integration," in *Proceedings of the Second International Interconnect Technology Conference* (1999), 161.
5. F Yang et al., "Investigation of Thermal Curing of an Organic Low-k Spin-On Dielectric by Variable-Angle Spectroscopic Ellipsometry" (paper presented at the 46th International Symposium of the American Vacuum Society, Seattle, October 25–28, 1999).

6. JA Woollam and PG Snyder, "Fundamentals and Applications of Variable Angle Spectroscopic Ellipsometry," *Materials Science and Engineering* B5 (1990): 279–283.
7. F Yang, M Tabet, and WA McGahan, "Characterizing Optical Properties of Red, Green, and Blue Color Filters for Automated Film Thickness Measurement," in *Proceedings of SPIE* 3332 (Bellingham, WA: International Society for Optical Engineering, 1998), 403–410.
8. WA McGahan et al., "Optical Characterization of TiN Thin Films," in *Proceedings of the ASMC* 9 (Piscataway, NJ: IEEE, 1996), 359–363.
9. WA McGahan, "Optical Characterization of Polycrystalline Silicon Thin Films," in *Proceedings o SPIE* 2725 (Bellingham, WA: International Society for Optical Engineering, 1996), 450–459.
10. VJ Coates, U.S. Pat. 5,045,704, 1991.

Feng Yang, PhD, is an applications scientist at Nanometrics in Sunnyvale, CA, specializing in optical dat analysis for the development of thin-film metrology applications. Before joining the company, he worked a staff scientist in the fields of ceramic thin-film deposition and device fabrication at Neocera (Beltsville, MD). He received a PhD in electrical engineering from the State University of New York at Buffalo in 1995. (Yang can be reached at 408/746-1600, ext. 183; or fyang@nanometrics.com.)

William A. McGahan, PhD, is chief scientist at Nanometrics. Before joining the company in 1995, he worked at J. A. Woollam (Lincoln, NE) in the area of development and applications development of spectroscopic ellipsometers. McGahan received BS, MS, and PhD degrees in electrical engineering from t University of Nebraska. He has published 46 papers on ellipsometry, magneto-optics, thermal characterization of materials, and semiconductor metrology; two chapters in textbooks on magneto-optical properties of materials and magneto-optical recording; and recently coauthored *Spectroscopic Ellipsometr and Reflectometry* with Harland Tompkins. (McGahan can be reached at 408/746-1600, ext. 123, or bmcgahan@nanometrics.com.)

Carol E. Mohler, PhD, is a research leader in the advanced electronics materials laboratory of Dow Chemical (Midland, MI). Since 1990 she has concentrated on the curing and oxidation of polymeric dielectric thin films. She received a BS in chemistry from the University of Michigan in Ann Arbor and a PhD in physical chemistry from the University of Wisconsin in Madison. (Mohler can be reached at 517/636-4770 or mohlerce@dow.com.)

Lisa M. Booms joined the advanced electronics materials laboratory of Dow Chemical in 1998. She is a process engineer supporting research and development of SiLK dielectric resin and supports customers on process issues. She received a BS from Saginaw Valley State University in University Center, MI. (Boom can be reached at 517/636-3667 or lmbooms@dow.com.)

Exhibit F 09/912,737

Addressing the challenges of spin-on low-k dielectric dispense management

Josh H. Golden, J. Eric Carrubba, and Jay Jung, *Microbar*

Optimizing dispense tool designs and SOD management will require cooperation between equipment manufacturers, materials suppliers, and end-users.

During the last five to eight years, the semiconductor industry, academia, and government labs have been engaged in an intense worldwide research effort in preparation for the integration of low-k dielectric materials in ICs at the 180-nm technology node, which was scheduled for first shipments in 1999. This effort was driven by the desire to uphold Moore's Law and the various revisions of the industry roadmap.[1–4] However, the transition from silicon dioxide films applied by chemical vapor deposition (CVD), which have a dielectric constant (k) value of 4.1 to 4.2, to inorganic, organic, and hybrid materials with k values of less than 3.0 has proven to be more difficult than predicted. Figure 1 illustrates the delayed adoption of low-k dielectrics based on the roadmaps.[4,5]

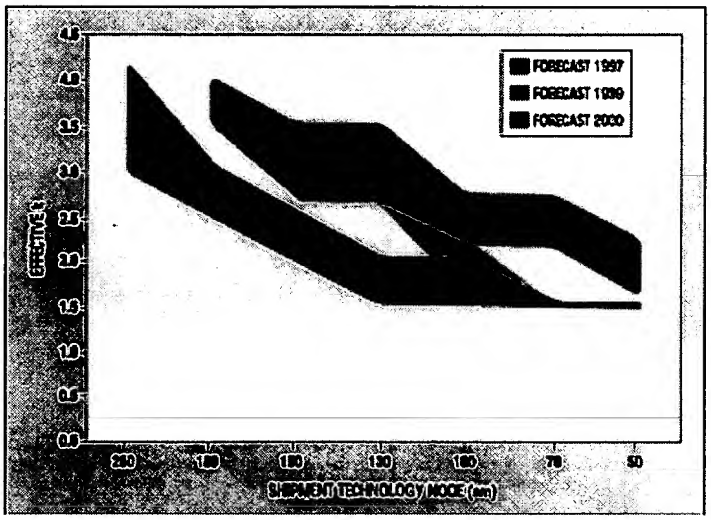

MicroMagazine.com
11444 W.Olympic Blvd.
Los Angeles, CA 90064
310.445.3700

Figure 1: The delayed implementation of low-k materials at each device generation. (Adapted from reference 5.)

As both research and delays continue, a debate has been raging over the choice of techniques for applying low-k materials. Both spin-on and CVD candidates present integration challenges because their properties differ from those of the benchmark, SiO_2, which is hard, relatively inert, thermally stable, and easy to deposit or grow.[6–8]

Table I compares the dielectric properties of SiO_2 to those of organic spin-on dielectrics (SODs) and $Si_wC_xO_yH_z$ CVD films. The organic SODs may present a greater integration challenge than do the hybrid $Si_wC_xO_yH_z$ CVD films, which are more "silica-like." For example, SiO_2 has a modulus of 72 GPa, while a leading polyarylene SOD exhibits a modulus of 2.7 GPa.[8] This approximately 27-fold difference in modulus has a significant effect on the efficacy of chemical mechanical planarization (CMP) processes, which subject copper interconnect layers to significant shear forces.[9]

Property	Material		
	Silicon Dioxide	Organic SODs	CVD SiwCxOyHz
Dielectric Constant (k)	3.9—4.5	2.4—2.85	2.5—3.2
Modulus (GPa)	72	2—3	4.2—10.8
Hardness (GPa)	8.7	~0.25	0.23—1.41
Composition	SiO2	Various: Poly(arylene ether) Poly(arylene) Poly(benzoxazole)	15—22% Si. 17—23% C, 18—30% O, 26—45%H

Table I: Comparison of some properties of silicon dioxide with those of SODs and carbon-doped siloxane film. (Adapted from reference 8.)

In addition to the modulus, heat dissipation is another important issue with low-k candidates, because their thermal conductivity is typically 20 to 30% lower than that of SiO_2.[6,7,10] Poor heat dissipation can cause localized metal-line heating, which eventually leads to device failure. Thermally induced stresses within the low-k film may lead to delamination because of mismatches between the film's coefficient of thermal expansion (CTE) and the substrate CTE. For example, silicon dioxide's CTE is 0.5 ppm/°C, aluminum's CTE is 23.1 ppm/°C, and copper's CTE is 16.5 ppm/°C. Because the CTE of many organic dielectrics is >50 ppm/°C, CTE mismatches can lead to high tensile stresses following thermal cycles.[7]

A successful low-k candidate must display several critical material properties: chemical resistance to oxidation and moisture absorption during plasma ashing, stripping and cleaning, and CMP processes; thermal stability (no weight loss or shrinkage following repeated

thermal stability (no weight loss or shrinkage following repeated isothermal soaks at 400°C); and the ability to adhere to substrates, including liners and barriers, in order to withstand the shearing and delamination forces exerted by the CMP process.

A variety of options have recently emerged to address some of the challenges associated with using low-k materials in ICs. These include delaying the implementation of such materials as well as new integration schemes. Approaches include:

- Combining new circuit architectures with aluminum and low-k dielectrics to achieve lower resistance-capacitance (RC) delays.[2,3,5,11]
- A fluorinated silica glass technique.
- An embedded approach that uses low-modulus and low-thermal-conductivity low-k materials only between the lines, where 80% of the reduced RC-delay benefit is realized. At the via level, SiO_2 or a spin-on glass (SOG) technique may be used for added strength and improved thermal conductivity.[5,12]
- Using a polyarylene thermoset at the lower five tight-pitch copper levels and fluorinated silica glass at the top three global wiring levels for strength and heat dissipation.[8,13]
- Using relatively inert ($k \sim 4.5$) silicon carbide as a CMP barrier film and hard mask to protect a potentially reactive low-k film.[6]

While these possibilities raise many interesting issues, this article focuses on some of the benefits and concerns associated with the adoption of SODs. The need for dispensing equipment especially designed for this application and the need for SOD material management capabilities are particularly emphasized.

SODs versus Hybrid CVD Films

The April 2000 announcement by IBM that it will adopt Dow Chemical's SiLK resin as an insulator for its dual-damascene copper processes at the 130-nm technology node represented the first major breakthrough in the spin-on versus CVD debate.[13] Since then, UMC in Hsinchu, Taiwan, and Altis Semiconductor (an IBM-Infineon joint venture) in Corbeil Essones, France, have announced that they will also use the 130-nm process technology developed with IBM, and it is likely that more companies will announce their adoption of SiLK sometime this year. However, other 2.2–3.1-k SODs are still being considered, including Honeywell's HOSP, a hybrid siloxane-organic polymer; Dow-Corning's XLK, a porous hydrogen silsesquioxane (HSQ); Schumacher's MesoELK, a porous silica product; and JSR's MSQ hybrid.

SODs' main competitors at the 130-nm technology node are hybrid $Si_wC_xO_yH_z$ CVD films with dielectric constants in the 2.5–3.0 range.

These films are more like SiO_2 than the SODs are, and they have a lower density and lower polarizability because of their pendant organic methyl groups. Other advantages of the films include the good availability and low cost of the precursor materials, as well as their ability to be processed with existing CVD tool sets.[5,14,15] However, the $Si_wC_xO_yH_z$ films are relatively soft compared to SiO_2 (0.23–1.41 versus 8.7 GPa).[8] It also appears that $Si_wC_xO_yH_z$ hybrids with a dielectric constant of <2.5 display film properties that will be inadequate for the 100-nm technology node, although research efforts are under way by materials and CVD tool suppliers to address such issues.

On the other hand, SODs have certain intrinsic material advantages over low-k CVD films. For example, a SOD material typically has a well-defined chemical composition that undergoes a specific and well-characterized physicochemical change (i.e., cross-linking) during thermal cure. In contrast, the composition of $Si_wC_xO_yH_z$ films may vary from recipe to recipe and from tool to tool, as a CVD process is developed and qualified.

In addition, because SOD compositions are created using established chemical synthesis and modification procedures, the preparation of porous materials with dielectric constants as low as 2.0 is readily achievable. A variety of approaches are being used by synthetic chemists in the preparation of both open- and closed-cell porous networks with optimized pore sizes and distributions. These include the use of porogens, such as a high-boiling-point solvent (Dow-Corning's XLK), or a thermally decomposable organic molecule, such as a dendrimer.[16]

Mesomorphous silicas represent another class of SODs. To create these materials, an organized porous silica or $Si_wC_xO_yH_z$ network is formed by templating silicon-containing precursors with organic surfactants in a mixed-solvent system. Sol-gel or sol-gel-like ordered structures are then created in a prebake step, followed by the burning off of the templating organic molecules. In contrast to these porous-SOD technologies, the preparation of porous materials for plasma deposition is a greater challenge because it is more difficult to control pore size, achieve pore-size homogeneity, and create closed-cell architectures. Both CVD equipment suppliers and materials manufacturers are researching ways to meet this challenge.

Another advantage of SODs over films applied by CVD is that the sensitivity of SODs to moisture, oxygen, and heat is generally understood and somewhat predictable. Thus, necessary precautions can be integrated into handling and dispensing procedures without extensive experimentation. The ease with which the handling and dispensing of these materials can be optimized, and the relative

simplicity of the spin-on process, help to hold down the end-user's cost of ownership (COO). In contrast to SODs, the optimization of $Si_wC_xO_yH_z$ processes requires rigorous experimental designs in order to achieve the best combination of mass flow and multiple-component precursor ratios, as well as the necessary process tool parameters. Significant effort must therefore be expended to maintain the process window, the cost of which typically has not been included in COO studies.[15] Another hidden cost is that incurred in the transference of the process from one site or tool to another, which can be difficult and time-consuming.

Proponents on both sides of the dielectric debate continue to argue the respective strengths and weaknesses of the various technologies, from materials properties to ease of use to COO.[15] However, it appears that a combination of SOGs, SODs, and CVD films will be used in conjunction with new integration schemes at both the 180- and 130-nm technology nodes, and possibly at the 100-nm node as well.

SOD Dispense Tool Design Issues

The implementation of SODs will require that new cooperative relationships be developed between tool manufacturers, materials suppliers, and end-users. Formerly, when spin-on tools were used only for photoresist, there was a mostly closed loop between spin-on track manufacturers and dispense cabinet providers. Now, however, because of a variety of factors, including the existence of multiple SOD candidates with different chemistries and their high costs (>$1000/L), it has become critical for equipment manufacturers, materials suppliers, and end-users to work closely to ensure that the chosen SOD will be optimally dispensed onto the wafer.

There are significant differences between photoresist dispense and SOD dispense that can affect tool design and process parameters. After dispense, a photoresist undergoes a variety of processes, including prebake, exposure, development, and cure, after which it is stripped off the wafer. But because an SOD is integrated permanently into the device structure, careful attention must be paid to preventing contamination and maintaining the correct material thickness and composition during the dispense process. Failure to control particles and other contaminants results in the classic "fly stuck in amber" scenario, which can ultimately lead to device failures.

In addition, while most photoresists can be handled similarly, each SOD has a different set of handling criteria because of its unique chemistry and physical properties. Dispense tool manufacturers must understand these properties and those of the carrier solvent(s), applying this knowledge to the design of their hardware and software. Knowledge of the SODs' properties must drive the choice of tool component materials and the integration of safeguards against

contamination. Table II lists some SODs and relevant information on their properties.

Property	SOD Material		
	Dielectric A	Dielectric B	Dielectric C
Dielectric constant (k)	2.65	2.0–2.5	2.5
Type (solute)	Polyarylene	Porous HSQ	Organic siloxane polymer
Solvent(s)	γ-Butyrolactone, cyclohexanone, mesitylene	2-Pentanone, toluene, tetradecane	Propyl acetate
Solute moisture sensitivity (25°C storage, 1 week)	No	No	Yes
Hygroscopic solvent(s)	Yes	Yes	Yes
Thermal sensitivity (25°C storage, 1 month)	No	Yes	Yes
Oxygen sensitivity (25°C storage, 1 week)	No	No	No
Particle formation potential (25°C storage, 1 week)	No	No	Yes
Flammable mixture	Yes	Yes	Yes

Table II: Comparative data on SOD properties that are useful in the design and operation of dispense tools. (Data collected from materials suppliers' material safety data sheets and and personal communications.)

Tool manufacturers must also consider the properties of SOGs and their derivatives, which may be used as etch stops and barriers in conjunction with a low-k SOD.[6,11] Because the wetting characteristics of SOGs typically are optimized for gap-fill and planarization applications, these materials are prone to wicking and may form small inclusions in nooks and crannies in the dispense apparatus' fluid path. This phenomenon can lead to the formation of cross-linked silica-like particles upon solvent removal or evaporation. One solution to this problem is to use low-roughness-average materials for the dispense tool's fluid paths and to provide a solvent-saturated inert-gas environment within the tool.

Many polar carrier solvents are hygroscopic or may undergo acid or base hydrolysis under certain conditions. While gross solvent hydrolysis is unlikely in a well-engineered dispense apparatus, even small amounts of moisture can have a deleterious effect on the composition of SODs that contain metastable siloxane oligomers or

composition of SODs that contain metastable siloxane oligomers of silane or siloxane adhesion promoters. Therefore, careful attention to SOD bottle changes and the use of an inert-gas backfill to prevent oxygen or moisture infiltration is required.

Some SOD materials are thermally sensitive and thus require a temperature-controlled environment to prevent spontaneous polymerization, cross-linking, or condensation of oligomeric moieties, which can result in particle formation. Possible measures to prevent such reactions and to optimize dispense temperature include transferring the cold-preserved SOD from the container to a secondary, temperature-controlled reservoir and the inclusion of thermal controls (±1°C) along the dispense tool's fluid path. Temperature control is important not only for preventing particle formation, but also for helping maintain the fluid viscosity necessary for correct on-wafer film thickness.

In addition to temperature controls, an effective SOD dispensing system should also provide solvent-saturated backfill and automated flush-purge capabilities for preventing particle formation and deposition within the dispense apparatus. While solvent-saturated backfill ensures a wetted path for the SOD with a like solvent or solvent mixture, an automatic solvent flushing protocol cleans the system and then dries it with an inert gas. An automated flush-purge system flushes and cleans dispense lines between batch changes and helps perform routine maintenance. The ability to isolate and purge portions of the fluid path for cleaning and servicing in a multitrack dispense tool while processing continues uninterrupted will become increasingly important as SOD end-users ramp up capacity and move from using 1-L containers to bulk delivery systems.

Another challenge facing SOD dispense systems is the removal of particles and microbubbles, which is accomplished through one-pass filtration or filtration with recirculation, depending on the material's requirements. A study of particle and microbubble removal using filtration with recirculation was conducted at the Honeywell Electronic Materials Star Center (Sunnyvale, CA) using a PMS M65 particle detector from Particle Measuring Systems (Boulder, CO) integrated with the Low-k 2.0 SOD/SOG dispense system from Microbar (Sunnyvale, CA).

In the study, the particle-size detection limit was 0.065 µm, and the dispense tool included a 0.065-µm filter. Data were collected at 25.5°C at a sampling flow rate of 0.6 ml/min. Figure 2 shows the results of this study for an $Si_wC_xO_yH_z$ hybrid SOD that is sensitive to both temperature and moisture and thus has the potential to form insoluble particles. As the figure indicates, acceptable particle reduction was achieved after approximately 3 hours, or 175 recirculation cycles. While it proved difficult to quantitatively differentiate microbubbles from particles because of their similar size and an inability to isolate each component, the study found that both particles and microbubbles

each component, the study found that both particles and microbubbles were removed to acceptable levels without affecting film thickness or quality.

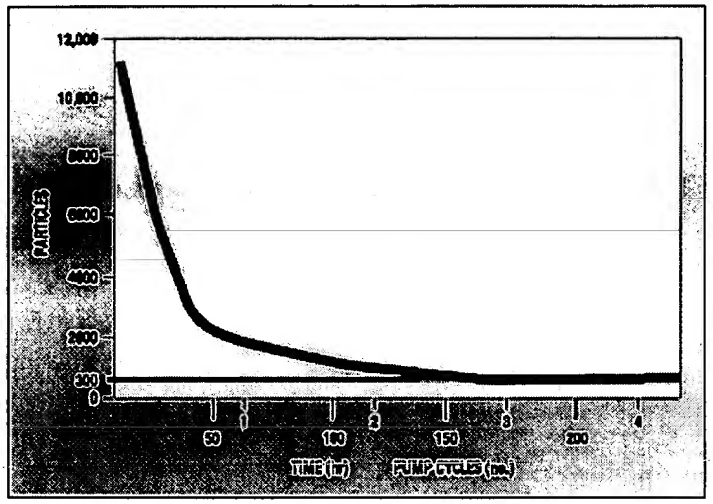

Figure 2: Data collected for an $Si_wC_xO_yH_z$ SOD hybrid using a particle detector that was integrated with an SOD dispense system equipped for filtration with recirculation.

Filter selection can be critical to achieving good results. While the choice of filter material and type is a materials-compatibility issue, the choice of pore size can directly affect SOD composition and molecular weight. Many SODs consist of oligomers or prepolymers and/or polymeric materials that have a specific molecular-weight distribution and average thermodynamic radius. A filter whose pore size is too small has the potential to fractionate this molecular-weight distribution and thus remove a certain population of oligomers or polymers from the SOD mixture. This can adversely affect the material's on-wafer thickness, physical properties, and, possibly, device yield performance. Because the molecular-weight distribution may also be affected by shearing forces (polymer chain cleavage), careful fluid-path design and selection of transfer pumps and associated apparatus are necessary for some SOD materials as well.

Dispense tool manufacturers also must address environmental safety and health concerns, including the prevention of spills and leaks of reactive, noxious, and flammable spin-on materials. Double-containment piping, spill sensors, quick-release fittings, and proper ventilation of and safe access to the dispense cabinet are among the features that can be included. Multiple-track SOD dispense schemes with built-in safety features can also increase tool efficiency and process uptime. Safety features that facilitate bottle change will also prove beneficial as SOD use increases.

SOD Management

The tracking and management of SODs is another important reason why materials suppliers, dispense tool manufacturers, and their

customers must develop cooperative relationships. Issues that affect an SOD's life span include supplier batch and materials information, the transport environment from the supplier to the end-user, and the dispense protocol and associated parameters. A combination of hardware and software strategies can be used to compile, manage, and share the required data. For example, SOD containers can include a wireless tracking device that operates in the RF spectrum and is located in a well or integrated in a dip tube. Activated at the SOD point of fill, the device logs such transport parameters as time, thermal history, shock, and tilt. Because some SODs are sensitive to temperature and shock, monitoring these parameters can pinpoint potential upsets that can lead to the spoilage of the material.

Batch-tracking capability is important for maintaining quality control, process stability, inventories, and orders. In a comprehensive SOD-tracking scheme, data collected at the point of fill, during shipment, at fab delivery, and before bottle installation in the dispense tool can be uploaded into a software package that allows analysis and the sharing of data among authorized users. Analytical features can include troubleshooting and go/no-go protocols to be implemented when an SOD shipment enters the fab receiving area and again during bottle changeover at the dispense tool. Wireless tracking can also be integrated with bar code schemes to enable analysis. Figure 3 illustrates a possible combination of hardware and software technologies that can serve as the anchors of an integrated system for the management of SODs.

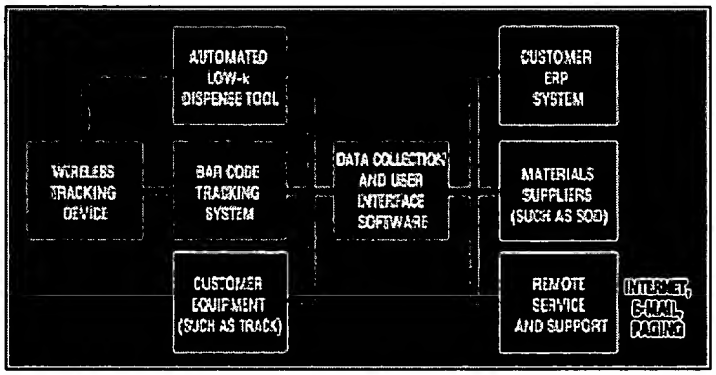

Figure 3: Schematic showing how a central software chemical-management package can link customers, materials suppliers, and dispense tool manufacturers with data from monitoring devices and process tools.

One example of such a system, developed by Microbar, includes the company's software platform and wireless tracking device. The software is capable of collecting data from the manufacturer's tool sets and those of other equipment suppliers, and can transmit both data and analytical results to materials suppliers and end-users via interfaces and the Internet. The types of information provided by the platform include histograms of equipment uptime and performance, maintenance and service logs, security information to be used by

process engineers to validate chemicals, and mass balances of chemical-distribution loops for environmental and operational expense measurements. The implementation of such a system should minimize equipment COO by promoting the efficient utilization of expensive SOD materials.

Conclusion

Although the debate over the optimal technique for applying low-k dielectrics continues, some semiconductor manufacturers have announced that they are adopting SODs. Such materials have several advantages over CVD films, including their well-defined chemical composition and physical characteristics. However, their adoption will require new cooperative relationships between equipment manufacturers, materials suppliers, and end-users. Tool designers, in particular, must understand the properties of the many available SOD materials to ensure that they are dispensed optimally. Dispense tools must be designed to enable the prevention and removal of contamination, and must have built-in safety features. SOD management schemes that link suppliers and customers will also be needed to minimize cost of ownership and facilitate the efficient use of the costly materials.

References

1. PV Zant, *Microchip Fabrication: A Practical Guide to Semiconductor Processing*, 4th ed. (New York: McGraw-Hill, 2000), 9.
2. TN Theis, "The Future of Interconnection Technology," *IBM Journal of Materials Research and Development* 44, no. 3 (2000): 379–390.
3. XW Lin and D Pramanik, "Future Interconnect Technologies and Copper Metallization," *Solid State Technology* 43, no. 10 (2000): 63–79.
4. *The International Technology Roadmap for Semiconductors*, (San Jose: Semiconductor Industry Association, 1999), 172–173.
5. L Peters, "Low-k Dielectrics: Will Spin-On or CVD Prevail?" *Semiconductor International* 23, no. 6 (2000): 108–124.
6. L Peters, "Solving the Integration Challenges of Low-k Dielectrics," *Semiconductor International* 22, no. 13 (1999): 56–64.
7. M Morgan et al., "Low Dielectric Constant Materials for ULSI Interconnects," *Annual Review of Materials Science* 30 (2000): 645–680.
8. JG Ryan et al., "Copper and Low-k Dielectric Integration Challenges," in *Proceedings of the Low-k Dielectric Materials Technology Conference, Semicon West* (San Jose: SEMI, 2000), A1–A5.
9. M Fury, "CMP Processing with Low-k Dielectrics," *Solid State Technology* 42, no. 7 (1999): 87–96.

10. J Wetzel, "An Evaluation of Low-k Materials for Interconnect Roadmap Requirements," in *Proceedings of the Low-k Dielectric Materials Technology Conference, Semicon West* (San Jose: SEMI, 2000).
11. T Hasegawa et al., "Copper Dual Damascene Interconnects with Low-k Dielectrics Using FLARE and an MSQ Hard Mask," in *Proceedings of the Low-k Dielectric Materials Technology Conference, Semicon West* (San Jose: SEMI, 2000): G1–G6.
12. H Kudo et al., "Copper Dual Damascene Interconnects with Very Low-k Dielectrics Targeting for 130-nm Node," in *Proceedings of the 2000 IITC* (San Francisco: IEEE, 2000), 270–272.
13. R Goldblatt et al., "A High Performance 0.13-µm Copper BEOL Technology with Low-k Dielectric," in *Proceedings of the 2000 IITC* (San Francisco: IEEE, 2000), 261–263.
14. R Laxman et al., "Synthesizing Low-k CVD Materials for Fab Use," *Semiconductor International* 23, no. 13 (2000): 95–102.
15. M Corbett and J Davis, "Tipping the Scales for Spin-On vs. CVD: Which Process Will Emerge as the Winner in Dielectric Polymer Technology?" *Semiconductor Magazine* 1, no. 9 (2000): 40–46.
16. C Hawker et al., "Supramolecular Approaches to Nanoscale Dielectric Foams for Advanced Microelectronic Devices," *Materials Research Society Bulletin* (April 2000): 54–58.

Josh H. Golden, PhD, is director of process technology at Microbar in Sunnyvale, CA. In that position, he is involved in the development of dispense solutions for low-k spin-on dielectrics and copper chemistries, and in the development of new technologies for the treatment of CMP wastewater. He was formerly a polymer chemist at Cytec Industries and lead chemist in the low-k dielectric materials program at Watkins-Johnson (now SVG). Golden has authored 20 papers and holds several patents in the areas of materials science and chemistry. He received a PhD in chemistry from Cornell University in Ithaca, NY. (Golden can be reached at 408/542-9069 or jgolden@microbar.com.)

J. Eric Carrubba is a project engineer at Microbar with more than 13 years of semiconductor equipment experience. Before joining the company, he was an engineering manager at the semi-gas equipment division of Matheson Tri-Gas. He received a BS in aeronautics from the engineering department of San Jose State University, in San Jose, CA. (Carrubba can be reached at 408/542-9061 or ecarr@microbar.com.)

Jay Jung is director of controls engineering at Microbar. Since 1988, he has worked in the pharmaceutical, paper, and semiconductor industries. He has expertise in bringing processing equipment from R&D to manufacturing and in implementing factorywide automation. He received a BS in electronic engineering from California Polytechnic State University in San Luis Obispo. (Jung can be reached

Polytechnic State University in San Luis Obispo. (Jung can be reached at 408/542-9072 or jjung@microbar.com.)

MicroHome | Search | Current Issue | MicroArchives
Buyers Guide | Subscribe to MICRO | Website Advertising Rates

Questions/comments about MICRO Magazine? E-mail us at feedback@micromagazine.com.

Exhibit G 09/912,737

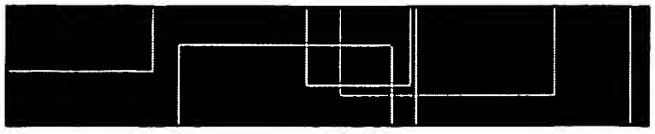

Product Showcase

Product Releases

REQUEST FREE PRODUCT INFO

Product Name:
Spin-on-Glass

Product Description:
ACCUGLASS T-11 Spin-on-Glass (SOG) Series is a family of methylsiloxanes that combine organic groups on an inorganic polymer backbone. It is used in production by IC manufacturers for interlevel and overcoat passivation smoothing. This product was designed for microelectronic applications requiring a high quality dielectric film of up to 3,500 Å, with a κ value of 3.8.

ACCUGLASS T-12B Spin-on-Glass (SOG) Series is a family of advanced spin-on dielectrics for use in the fabrication of integrated circuits. Chemically, this product belongs to the methylsiloxane family of polymers. This crack-resistant material features one-half micron single coat thicknesses, low shrinkage upon cure, and a κ value of 3.1.

ACCUGLASS T-14 Spin-on-Glass (SOG) series is a family of siloxane polymers formulated to fill narrow, high aspect ratio spaces without voiding and to more completely planarize multi-level metal devices. The organic content of the material is approximately 10%. With a κ value of 3.8, this material has good adhesion to silicon, thermal oxide, CVD oxide and aluminum. This polymer is formulated for microelectronic applications to better planarize all ICs, to fill narrow gaps in 0.5 µm to 0.35 µm devices and to extend the use of SOG for next generation ICs.

By: Honeywell

LIST YOUR COMPANY

Send This Page To An Associate